AIIM

Association for Information and Image Management

1100 Wayne Avenue, Suite 1100
Silver Spring, Maryland 20910
301/587-8202

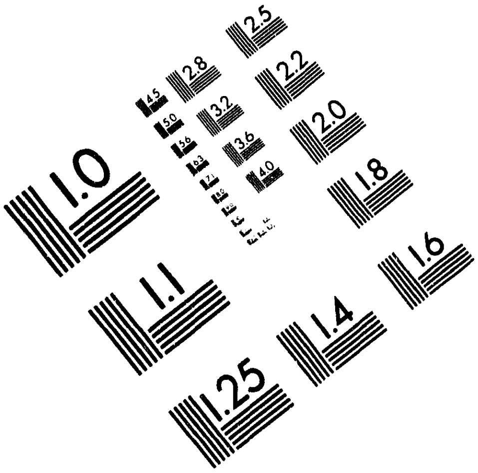

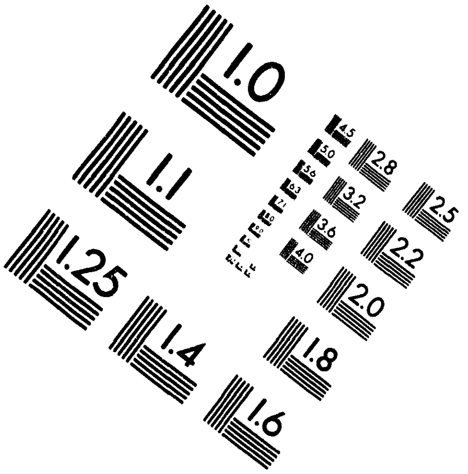

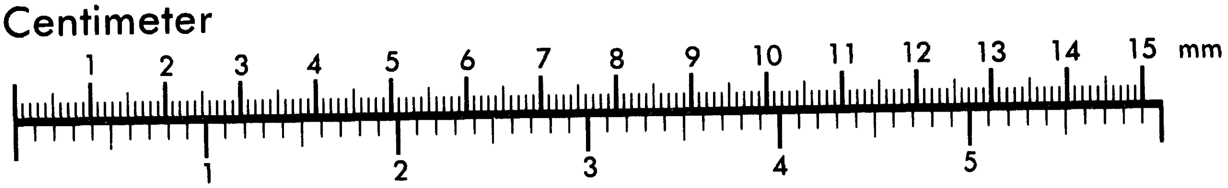

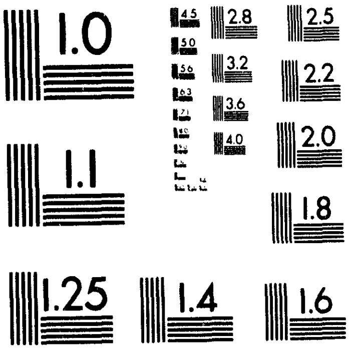

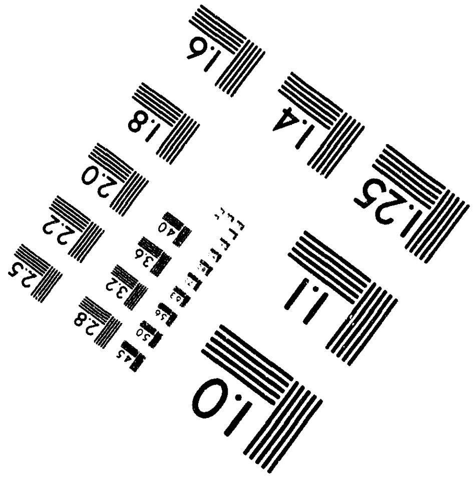

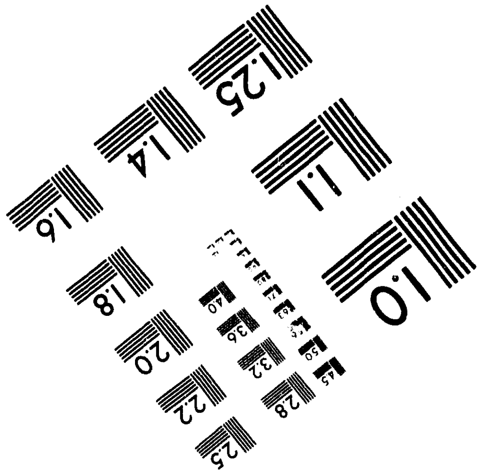

MANUFACTURED TO AIIM STANDARDS
BY APPLIED IMAGE, INC.

1 of 1

12/5-94 JSO ①

UCRL-ID-115768

Study of Cesium Volatility from Sodium Carbonate Based Melts

Bartley B. Ebbinghaus
Oscar H. Krikorian
Martyn G. Adamson
Dennis L. Fleming

December 1993

Lawrence
Livermore
National
Laboratory

Work performed under the auspices of the U.S. Department of Energy by the Lawrence Livermore National Laboratory under Contract W-7405-ENG-48.

Available to DOE and DOE contractors from the
Office of Scientific and Technical Information
P.O. Box 62, Oak Ridge, TN 37831
Prices available from (615) 576-8401, FTS 626-8401

Available to the public from the
National Technical Information Service
U.S. Department of Commerce
5285 Port Royal Rd.,
Springfield, VA 22161

Study of Cesium Volatility from Sodium Carbonate Based Melts

Bartley B. Ebbinghaus
Oscar H. Krikorian
Martyn G. Adamson
Dennis L. Fleming

Lawrence Livermore National Laboratory
Livermore, CA 94551

Table of Contents

Study of Cesium Volatility from Sodium Carbonate Based Melts

Bartley B. Ebbinghaus
Oscar H. Krikorian
Martyn G. Adamson
Dennis L. Fleming

Lawrence Livermore National Laboratory
Livermore, CA 94551

Abstract

The purpose of this study was to obtain thermodynamic data on cesium volatility from sodium carbonate based molten salts for application to the Rockwell-ETEC molten salt oxidation process. At temperatures ranging from 1073 to 1373 K, volatility tests were conducted on a horizontal and a vertical transpiration apparatus using a carrier gas composed of $CO_2(g)$ and $H_2O(g)$ which was passed over or bubbled through a sodium carbonate bath containing cesium carbonate and various additives. The major vapor species was identified to be CsOH(g) except when greater than 3% chloride is present in the melt, then the major vapor species is CsCl(g). The decrease in volatility of cesium as a function of cesium concentration in Cs_2CO_3-Na_2CO_3 mixtures follows Raoult's law very closely. Thus, this system exhibits close to ideal solution behavior. The addition of 22.5 wt% sodium sulfate decreases the cesium volatility by just under a factor of 2, and the addition of 10.0 wt% sodium chloride increases the cesium volatility about an order of magnitude. The addition of 2.0 wt% ash, molecular sieve, or silica show little or no effect. However, the data indicate that higher concentrations of ash will decrease the cesium volatility. For the addition of 22.5 wt% sodium sulfate the activity coefficient, $\gamma(Cs_2CO_3)^{1/2}$, is calculated to be 0.720 ± 0.068, and for the addition of 10.0 wt% sodium chloride, the activity coefficient, $\gamma(CsCl)$, is calculated to be 8.118 ± 2.317. Assuming that Henry's law applies, these activity coefficients are used to extrapolate the effect on cesium retention in the molten salt oxidizer of sulfate and chloride at lower cesium concentrations.

Introduction

This study has been performed in support of the Rockwell-ETEC molten salt oxidation process. In the Rockwell process, a combustible waste material is fed along with excess air into a salt bath composed primarily of sodium carbonate which is typically kept between 1150 and 1250 K. This oxidizes the waste material to yield primarily carbon dioxide, water vapor, and an ash residue which is wetted and retained by the melt. Except for carryover due to volatility, physical entrainment, or splashing, any hazardous metals, actinides, and fission products in the waste feed are held up and retained by the melt.

During the fall of 1992, Rockwell-ETEC tested the molten salt oxidation process by destroying 50 gallons of radioactively contaminated oil [1]. As well as actinides and other fission products, the oils contained radioactive cesium, ^{137}Cs, which is a major fission product of both uranium and plutonium and has a half-life of about 30 years. Rockwell's data from the oil processing indicated that only 53% of the radioactive cesium was retained in the melt when a sodium carbonate bath was used and only 85% of the radioactive cesium was retained in the melt when a bath mixture of sodium carbonate and sodium sulfate was used. Previous work with non-radioactive cesium [2] showed much greater cesium retention in the molten salt oxidizer, i.e. greater than 99.5%. The cesium in the waste feed was present as cesium nitrate and the waste feed was composed of a mixture of approximately 50wt% paper, 8wt% PVC, 32wt% polyethylene, and 10wt% rubber. The reason for the large discrepancy between Rockwell's older and more recent data is unknown. In the earlier work, 16 wt% ash was present in the carbonate melt which may have interacted with the cesium and reduced its volatility. Earlier work was also conducted at lower temperatures, about 1153 K, whereas more recent work was conducted at higher temperatures, about 1198 K.

The goal of this study has been to provide cesium volatility data from molten carbonate based salts under a variety of conditions such that the effects of operating conditions on cesium retention in the molten salt oxidizer can be better understood. In this work, the major cesium vapor species have been identified, and the effects of cesium concentration and additives (sulfate, chloride, and ash) on cesium volatility have been measured.

Table 1. Thermodynamic functions for $Cs_2CO_3(s,l)$.

S°_{298} = 212.73 ± 1.42 J/mol-K
$\Delta H^\circ_{f,298}$ = -1134.93 ± 0.63 kJ/mol
$S^\circ_{fus,1061}$ = 46.370 J/mol-K
$\Delta H^\circ_{fus,1061}$ = 49.199 kJ/mol

T (K)	Cp (J/mol-K)	S°_T (J/mol-K)	$-(G^\circ_T-H^\circ_{298})/T$ (J/mol-K)	$H^\circ_T-H^\circ_{298}$ (kJ/mol)
298.15	123.830	212.732	212.732	0.000
300	124.110	213.499	212.734	0.229
400	136.371	250.992	217.764	13.291
500	145.771	282.463	227.638	27.412
600	154.043	309.782	239.101	42.409
700	161.784	334.124	250.966	58.203
800	169.241	356.207	262.761	74.756
900	176.534	376.563	274.289	92.046
1000	183.724	395.535	285.475	110.060
1061(s)	188.360	406.541	292.120	121.400
1061(l)	195.138	452.911	292.120	170.599
1100	195.138	459.955	297.947	178.209
1200	195.138	476.934	312.165	197.723
1300	195.138	492.554	325.449	217.237
1400	195.138	507.015	337.907	236.751
1500	195.138	520.478	349.635	256.265
1600	195.138	533.072	360.711	275.778
1700	195.138	544.903	371.201	295.292
1800	195.138	556.056	381.164	314.806
1900	195.138	566.607	390.649	334.320
2000	195.138	576.616	399.699	353.834

Background Studies

Vapor Species above $Cs_2CO_3(l)$ and $CsCl(l)$:

A considerable amount of thermodynamic data are already available for cesium compounds and vapor species which might be important in the molten salt oxidation process. Data for Cs(g), $Cs_2(g)$, $Cs_2O(g)$, CsO(g), $Cs_2O_2(g)$, CsOH(g), and $Cs_2(OH)_2(g)$ are given by Cordfunke and Konings [3], data for $CsO_2(g)$ are given by Lamoreaux and Hildebrand [4], and data for CsCl(l), CsCl(g) and $Cs_2Cl_2(g)$, are given in the JANAF tables [5]. However, thermodynamic data for cesium carbonate, $Cs_2CO_3(s,l)$, are limited. The heat capacity of the solid is given by Barin [6], the $\Delta H°_{f,298}$ value is given by Johnson and Gayer [7], and the $S°_{298}$ value is determined from volatility data given later in this study. The enthalpy of fusion, $\Delta H°_{fus}$, is given by Kobayasi, et al. [8]. They also give the melting point as 1061 K. A best estimate for the heat capacity of the liquid was made by averaging available heat capacities for all the molten alkali carbonate and sulfate salts [5,6]. The resulting thermodynamic functions, C_p, $S°_T$, $-(G°_T - H°_{298})/T$, and $H°_T - H°_{298}$, calculated for $Cs_2CO_3(s,l)$ are given in Table 1.

From these data, the vapor species above $Cs_2CO_3(l)$ and CsCl(l) can be calculated. To approximate conditions present in the molten salt oxidizer, $p(O_2)$ and $p(H_2O)$ are each taken to be 0.10 atm. The logarithm of the vapor pressures of the various elemental, oxide, and hydroxide species above $Cs_2CO_3(l)$ are given in Figure 1. Clearly, CsOH(g) is the major vapor species followed by $Cs_2(OH)_2(g)$. The logarithm of the vapor pressure of the chloride species above CsCl(l) are given in Figure 2. For comparison, the hydroxide species formed above $Cs_2CO_3(l)$ are also shown. Here, CsCl(g) is the major chloride vapor species. In addition, the vapor pressure of CsCl(g) above CsCl(l) is about an order of magnitude greater than the vapor pressure of CsOH(g) above $Cs_2CO_3(l)$. Thus, the thermodynamic data indicate that CsOH(g) is the major vapor species in the molten salt oxidizer except when sufficient chloride is present, then CsCl(g) is the major vapor species.

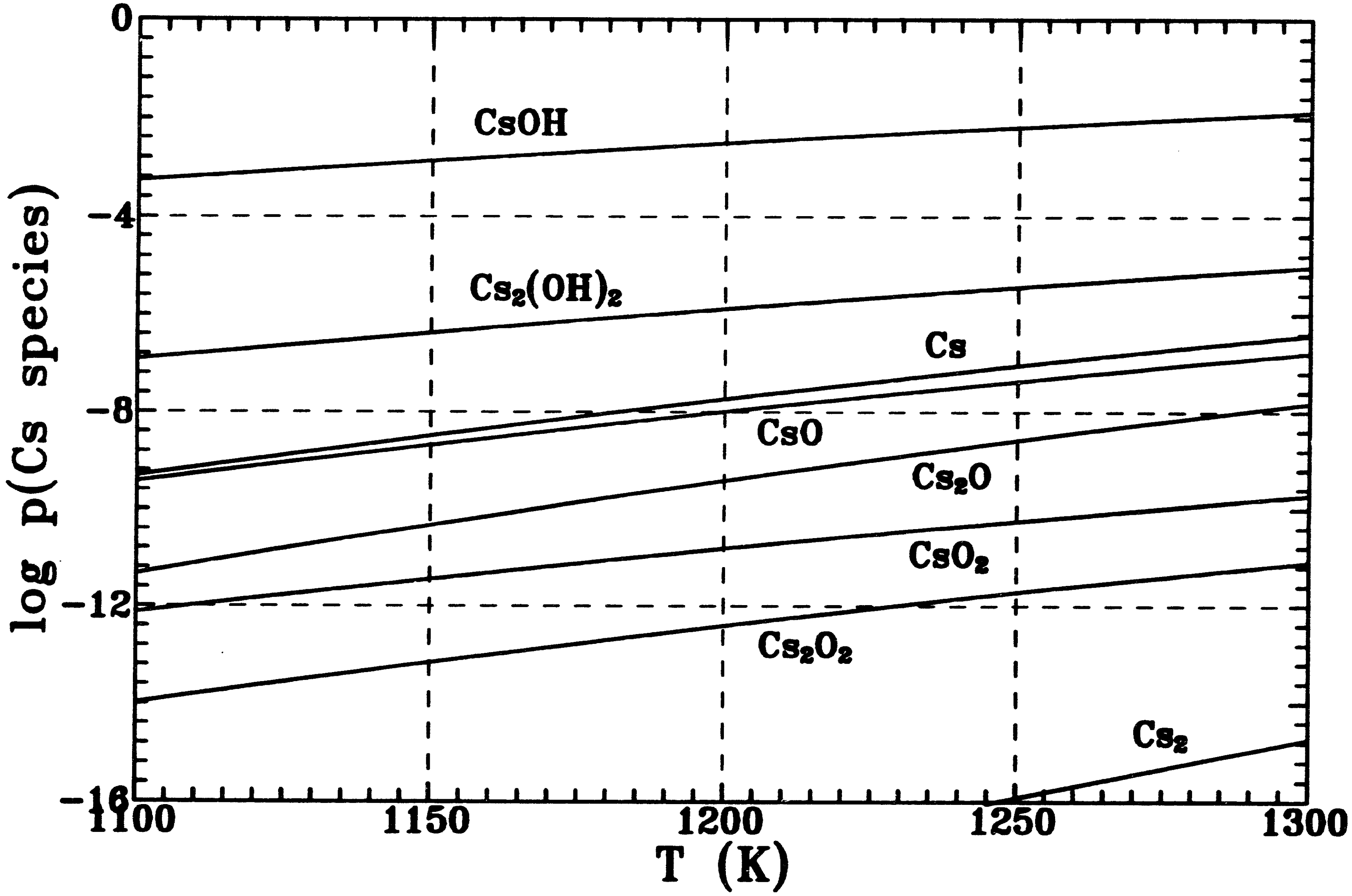

Figure 1. Plot showing the logarithm of the elemental, oxide, and hydroxide species vapor pressures formed above $Cs_2CO_3(l)$ as a function of temperature with $p(O_2)$, $p(H_2O)$, and $p(CO_2)$ each at 0.10 atm.

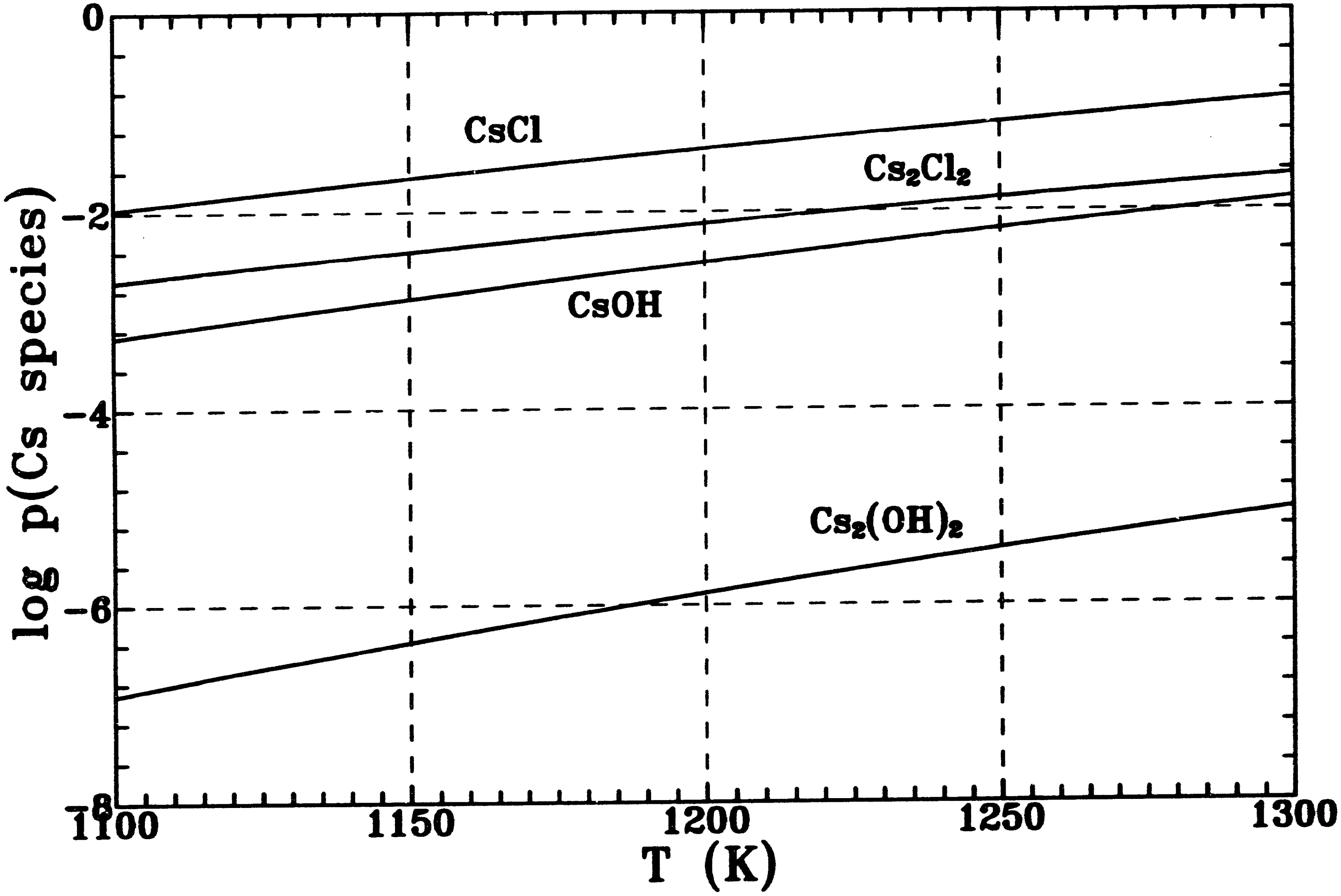

Figure 2. Plot showing the logarithm of the chloride species vapor pressures formed above CsCl(l) and the logarithm of the hydroxide species vapor pressures formed above Cs_2CO_3(l) as a function of temperature with p(O_2), p(H_2O), and p(CO_2) each at 0.10 atm.

Calculated Activity Coefficients in Various Salt Systems:

Since cesium will be present in the carbonate bath as a solution in sodium carbonate, the activity of the cesium salt, Cs_2CO_3, Cs_2SO_4, or CsCl, is needed to calculate its volatility. The activity of the cesium salt is given by

$$a(Cs_2CO_3) = \gamma(Cs_2CO_3)y^+(Cs^+)^2y^-(CO_3^{2-}), \qquad (1)$$

$$a(Cs_2SO_4) = \gamma(Cs_2SO_4)y^+(Cs^+)^2y^-(SO_4^{2-}), \qquad (2)$$

or

$$a(CsCl) = \gamma(CsCl)y^+(Cs^+)y^-(Cl^-) \qquad (3)$$

where $y^+(Cs^+)$ is the cation equivalent fraction of cesium and $y^-(CO_3^{2-})$, $y^-(SO_4^{2-})$, and $y^-(Cl^-)$ are the anion equivalent fractions of carbonate, sulfate, and chloride. The cation equivalent fraction of component A in a binary salt system is defined as

$$y^+(A) = q(A)x^+(A)/[q(A)x^+(A) + q(B)x^+(B)] \qquad (4)$$

where $x^+(A)$ and $x^+(B)$ are the cation mole fractions of substances A and B, and q(A) and q(B) are the ionic charges of A and B. If the charges are the same, then the equivalent fraction equals the mole fraction. If y^- and x^- are substituted for y^+ and x^+, the same equation defines the anion equivalent fraction. The cation mole fraction of component A is defined as

$$x^+(A^+) = N(A)/[N(A) + N(B)] \qquad (5)$$

where N(A) is the number of moles of cation A and N(B) is the number of moles of cation B. The anion mole fraction is defined in a similar manner. The reason that the activities of the salts are related to the product of the cation and anion equivalent fractions in the molten salt rather than the product of the cation and anion mole fractions is a result of the fact that vacancies are associated with anions or cations of greater charge in order to maintain charge neutrality. In an NaCl crystal lattice, for example, one Ca^{2+} ion and substitutes for two Na^+ ions leaving a vacancy in place of one of the Na^+ ions.

The activity coefficients for Cs_2CO_3, Cs_2SO_4, and CsCl have not yet been determined from volatility measurements, but some enthalpy of solution data exists [9-11] for which the activity coefficients of Cs_2CO_3 in Na_2CO_3(l), Cs_2SO_4 in Na_2SO_4(l), and CsCl in NaCl(l) can be calculated. The enthalpies of mixing for these three binary systems are given in Table 2. Assuming an ideal entropy of mixing and either a common cation or a common anion, the activity coefficient of component A at infinite dilution of A in a solution of B is given by

$$RT\ln\gamma^{\infty}(A) = 1/2[\Delta H_{mix}/y(A)y(B)]. \qquad (6)$$

For Cs_2CO_3 in Na_2CO_3(l), Cs_2SO_4 in Na_2SO_4(l), and CsCl in NaCl(l), the activity coefficients at infinite dilution, $\gamma(Cs_2CO_3)^{1/2}$, $\gamma(Cs_2SO_4)^{1/2}$, and γ(CsCl), at 1200 K are calculated to be 0.656, 0.835, and 0.701, respectively. Since each of the activity coefficients are not reduced greatly from unity, each of these solutions does not deviate greatly from ideal solution behavior.

Each of the above solutions have a common anion. Thus, the effect on activity coefficients of mixing of different anions should also be considered. Enthalpy of mixing data for the systems Na_2CO_3(l)-Na_2SO_4(l), Na_2SO_4(l)-NaCl(l), and Na_2CO_3(l)-NaCl(l) have been calculated [12,13]. These data, derived primarily from optimized phase diagram data, are given in Table 3. The interaction in these systems is also weak. Using eqn (6), the activity coefficients at infinite dilution for Na_2CO_3 in Na_2SO_4(l) ($\gamma(Na_2CO_3)^{1/2}$), Na_2SO_4 in Na_2CO_3(l) ($\gamma(Na_2SO_4)^{1/2}$), Na_2CO_3 in NaCl(l) ($\gamma(Na_2CO_3)^{1/2}$), NaCl in Na_2CO_3(l) (γ(NaCl)), Na_2SO_4 in NaCl(l) ($\gamma(Na_2SO_4)^{1/2}$), and NaCl in Na_2SO_4(l) (γ(NaCl)) are calculated to be 1.000, 1.000, 1.051, 1.051, 1.157, and 1.112, respectively. Each of these activity coefficients are not greatly different from unity, thus each of these solutions does not deviate greatly from ideal solution behavior. For solutions containing cesium rather than sodium, the behavior is expected to be similar.

A last possibility are solutions where neither anions nor cations are common. No data exits which allows activity coefficients to be calculated. However, some indication of the activity coefficient values can be gained by considering the exchange reactions

$$Cs_2CO_3(l) + Na_2SO_4(l) = Cs_2SO_4(l) + Na_2CO_3(l), \qquad (7)$$
$$K_{eq} = \gamma(Na_2CO_3)\gamma(Cs_2SO_4)/\gamma(Cs_2CO_3)\gamma(Na_2SO_4)$$

Table 2. Enthalpies of mixing for cesium and sodium binary molten salt systems.

$\Delta H_{mix}/[x^{+}(Cs^{+})x^{+}(Na^{+})] = a + bx^{+}(Na^{+})$, kJ/mol

$x^{+}(Cs^{+})$ = mole fraction of cesium salt
$x^{+}(Na^{+})$ = mole fraction of sodium salt

system	a	b	ref.
$Na_2CO_3(l)$-$Cs_2CO_3(l)$	-8.89	0.47	[7]
$Na_2SO_4(l)$-$Cs_2SO_4(l)$	-4.31	0.71	[8]
$NaCl(l)$-$CsCl(l)$	-3.22	-0.33	[9]

Table 3. Enthalpies of mixing for various sodium containing binary molten salt systems.

$\Delta H_{mix}/[y^{-}(A)y^{-}(B)] = a + b[y^{-}(B) - y^{-}(A)]$, kJ/equivalent

$y^{-}(A)$ = anion equivalent fraction of component A
$y^{-}(B)$ = anion equivalent fraction of component B

system A - B	a	b	ref.
$NaCl(l)$-$Na_2CO_3(l)$	0.498	0.0	[10]
$NaCl(l)$-$Na_2SO_4(l)$	1.256	0.197	[10]
$Na_2CO_3(l)$-$Na_2SO_4(l)$	0.0	0.0	[11]

$$Cs_2CO_3(l) + 2\ NaCl(l) = 2\ CsCl(l) + Na_2CO_3(l), \qquad (8)$$
$$K_{eq} = \gamma(Na_2CO_3)\gamma(CsCl)^2/\gamma(Cs_2CO_3)\gamma(NaCl)^2$$

and

$$Cs_2SO_4(l) + 2\ NaCl(l) = 2\ CsCl(l) + Na_2SO_4(l) \qquad (9)$$
$$K_{eq} = \gamma(Na_2SO_4)\gamma(CsCl)^2/\gamma(Cs2SO4)\gamma(NaCl)^2$$

The equilibrium constants are given in terms of activity coefficients only because the equivalent fractions of the anions and cations drop out of the equations. Taking the thermodynamic functions for $CsCl(l)$, $NaCl(l)$, $Na_2CO_3(l)$, and $Na_2SO_4(l)$ from the JANAF tables [5], the thermodynamic functions for $Cs_2SO_4(l)$ from Barin [6], and the thermodynamic functions for $Cs_2CO_3(l)$ given herein (Table 1), the equilibrium constant for each of the above reactions can be calculated. At 1200 K, the equilibrium constants are calculated to be 6.16, 93.8, and 15.2, respectively. Thus, the products in reactions (7) to (9) are more stable than the reactants and the activity coefficients of the products are greater than the activity coefficients of the reactants.

Experimental

Transpiration Method:

In the transpiration method [14], a known amount of carrier gas is slowly passed over a solid or bubbled into a liquid in a furnace chamber, such that any volatile gases produced become entrained in the carrier gas and are swept out of the chamber where the volatilized material then condenses on a substrate and is analyzed. The carrier gas may also contain reactive gases that are important in controlling the formation of the vapor species. For these experiments, $CO_2(g)$ and $H_2O(g)$ are the reactive gases. Variation of flow rate of the carrier gas permits one to establish the range of flow rates under which the carrier gas becomes saturated with the equilibrium vapor pressure of the volatilizing material. If the flow rate is too slow, then diffusional transport of the saturated vapor dominates over entrainment by the carrier gas. A vapor pressure which is apparently higher than the saturated equilibrium vapor pressure will result. If the flow rate is too high, the residence time of the carrier gas is not long enough to obtain saturation of the volatile material. A vapor pressure which is apparently lower than the saturated equilibrium vapor pressure will result. At intermediate flow rates, the residence time of the carrier gas is long enough such that the carrier gas is saturated with the volatile material, but short enough such that transport by gaseous diffusion is insignificant. This is the region in which the apparent vapor pressure equals the saturated equilibrium vapor pressure and is called the "plateau" region because a plot of apparent vapor pressure as a function of flow rate will be flat over this region with a rise in the curve at low flow rates and a drop in the curve at high flow rates.

The transpiration method also allows one to obtain the formula for the volatilizing species by varying the pressures of the reactive gases. In the case of cesium, the major vapor species above the carbonate based salt are expected to be either CsOH(g) or CsCl(g) which are given, respectively, by the reactions and the equilibrium constants

$$1/2\ Cs_2CO_3(l) + 1/2\ H_2O(g) = CsOH(g) + 1/2\ CO_2(g) \qquad (10)$$
$$K_{eq} = p(CsOH)p(CO_2)^{1/2}/p(H_2O)^{1/2}a(Cs_2CO_3)^{1/2}$$

and

$$CsCl(l) = CsCl(g) \qquad (11)$$
$$K_{eq} = p(CsCl)/a(CsCl).$$

From the equilibrium constant expression for reaction (10), the CsOH(g) pressure is inversely dependent upon the square root of the $CO_2(g)$ pressure and directly dependent upon the square root of the $H_2O(g)$ pressure. Other pressure dependencies would indicate other species. For reaction (11), the CsCl(g) pressure will be independent of the $CO_2(g)$ and $H_2O(g)$ pressures.

Description of Transpiration Equipment:

In order to conduct the cesium volatility experiments, two transpiration apparatuses were used, a horizontal arrangement and a vertical arrangement. The horizontal apparatus is a modified version of that used previously for the uranium oxide volatility measurements [15]. This unit was used for the cesium in ash experiments, for some experiments on pure cesium carbonate, and for some experiments on a cesium carbonate and sodium carbonate mixture. The horizontal unit is illustrated schematically in Figure 3. The furnace is a Marshall furnace with Pt/Rh windings, rated to 1450°C in air, and has a uniform temperature hot zone about 17 cm long. The furnace tube was alumina, 4.5 cm OD by 60 cm long. Stainless steel end caps designed with Viton

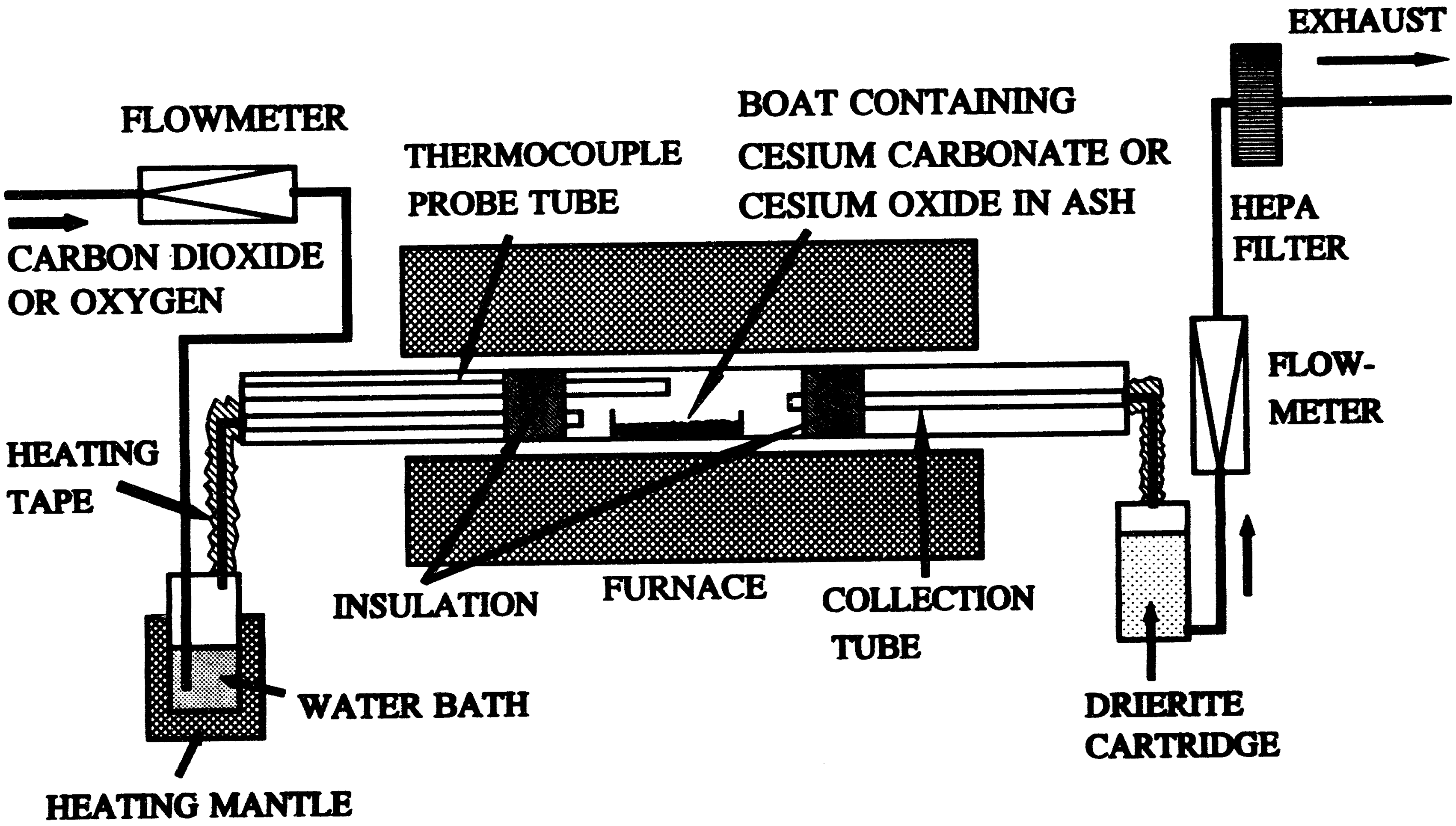

Figure 3. Schematic diagram of the horizontal transpiration apparatus.

o-ring seal compression fittings were used to seal off the ends of the furnace tube. From the upstream side, a gas inlet tube extended through a Viton o-ring seal compression fitting on a stainless steel end cap, through two alumina disks, 4.5 cm diameter by 3 mm thick, holding between them about 6 cm of Kaowool insulation (53wt% SiO_2 and 47wt% Al_2O_3) and to the border of the hot zone. The alumina disks and insulation were used to better define the hot zone. The thermocouple protection tube ran parallel to the gas inlet tube and also extended through a Viton o-ring seal compression fitting in the end cap, through the two alumina disks and insulation, and to the center of the hot zone. From the down stream side, a fused silica exit tube, 6 mm OD, extended through a Viton o-ring seal compression fitting on the other stainless steel end cap, through two additional alumina disks, 4.5 cm diameter by 3 mm thick, holding another 6 cm of Kaowool insulation, and to the border of the hot zone. The gas exit tube served as a collector tube for deposition of volatilized cesium and is referred to hereafter as the collection tube. Platinum boats, 2.5 cm wide by 6 cm long by 1 cm high, were used to contain the ash and the carbonate samples. For most of the runs using carbonate samples, the inside of the furnace tube in the hot zone and the alumina disks at the edge of the hot zone were lined with platinum foil, 0.08 mm thick, to minimize any reaction of the cesium vapor with the alumina walls. Temperatures were measured by a type-S thermocouple which was assumed to be accurate to within ± 2°C based on previous checks made with two other type-S thermocouples [15].

The vertical apparatus is similar in many ways to the horizontal apparatus. The vertical unit is illustrated schematically in Figure 4. This unit was used for the bulk of the experiments on carbonate based melts. Again, the furnace is a Marshall furnace with Pt/Rh windings, rated to 1450°C in air, and has a uniform temperature hot zone of about 12 cm in the vertical position. The furnace tube was alumina, 7 cm OD by 47 cm long, and closed on the bottom end. A stainless steel end cap designed with a Viton o-ring compression seal fitting was used to seal off the top end of the furnace tube. Two alumina tubes, a 9 mm OD gas inlet tube and a 9 mm OD thermocouple protection tube, and one, 9 mm OD, fused silica tube for sample collection and gas outlet, were extended through Viton o-ring compression seal fittings on the stainless steel endcap, through two alumina disks, 6 cm diameter by 4 mm thick, holding between them about 10 cm of Kaowool insulation. The gas inlet tube and the thermocouple protection tube were extended down into the carbonate melt about 1 cm

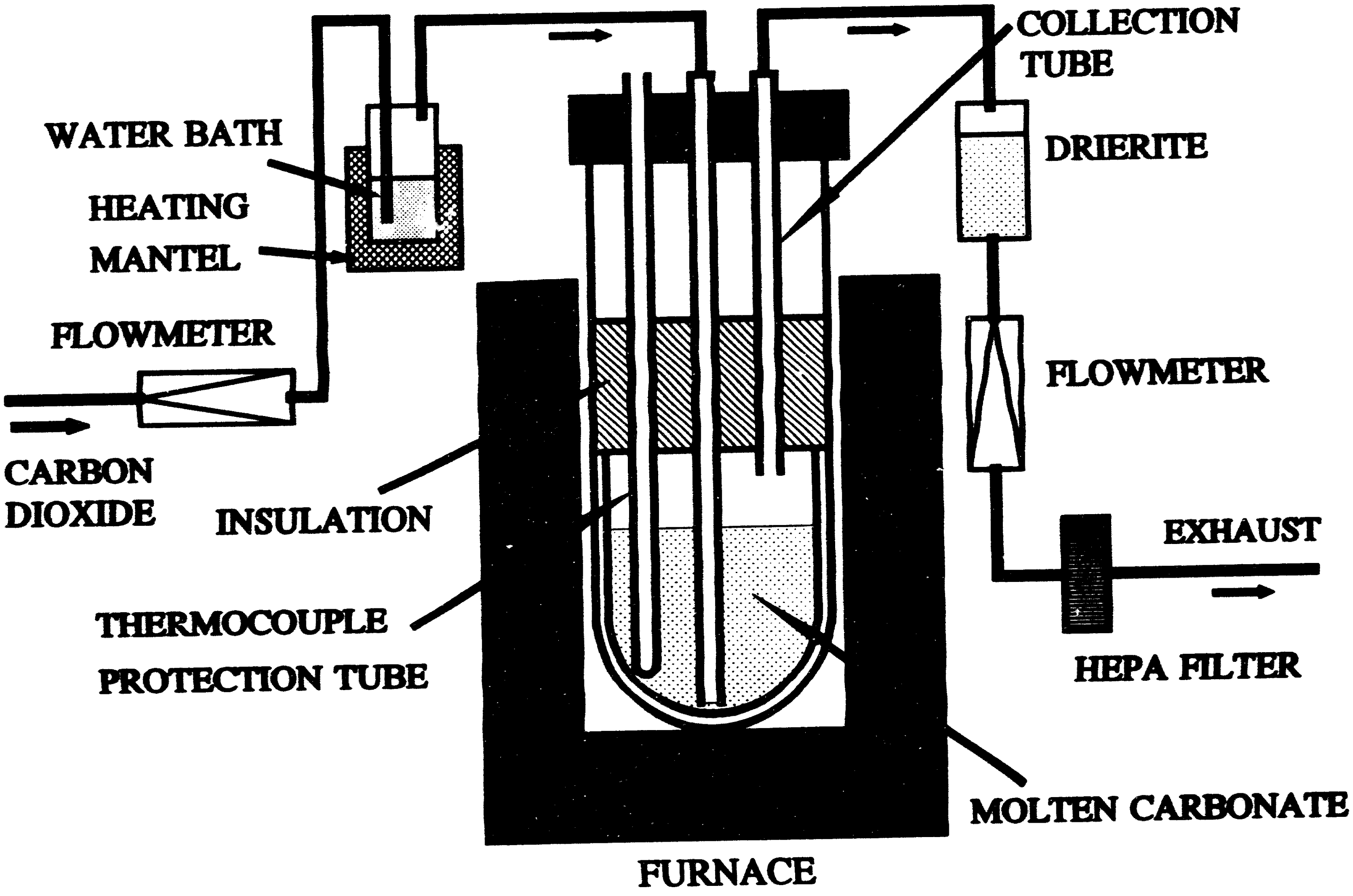

Figure 4. Schematic diagram of the vertical transpiration apparatus.

from the bottom. The collection tube was extended only to the end of the hot zone in the gas space above the melt. A round bottom alumina crucible, 5.9 cm OD by 15.3 cm high, was used to contain the carbonate melt. Temperatures were measured either by a type-S or a type-K thermocouple. In each experiment a back-up type-K thermocouple was also used which never differed by more than 3°C from the primary thermocouple.

In both the horizontal apparatus and the vertical apparatus, a water saturator was located upstream of the furnace. The water saturator was made of a 6-mm-thick wall aluminum vessel with an 800 cm^3 capacity and provided with a fritted stainless steel disperser for the carrier gas which was located 1 cm above the bottom of the vessel. The water level in the saturator was typically 500-600 cm^3 during the runs and the vessel was heated by a Glas-col mantle. A desiccant cartridge filled with Drierite ($CaSO_4$) was located downstream of the furnace. This cartridge was removed and weighed before and after an experiment to determine the total amount of water transported. All gas lines were stainless steel. Valves were also stainless steel with Viton rubber seals. Stainless steel compression fittings with Viton o-ring seals were used to connect the inlet and collection tubes to the gas lines. Briskheat silicone rubber heating tapes were wrapped around the lines leading from the water saturator to the furnace and from the furnace to the desiccant and maintained at around 150°C in order to prevent water vapor from condensing in the lines. Precision Flow devices PFD-401 mass flow controllers were used to control $O_2(g)$ and $CO_2(g)$ flow inputs and to monitor the gas flow output. The input flow controllers were calibrated by the supplier for $O_2(g)$. The readings were measured in cm^3/min of $O_2(g)$ at stp. The capacity of the flow controller was 50 cm^3/min for the ash experiments and 100 cm^3/min for all other experiments. The accuracy of the mass flow controller is ± 1% of the full scale reading and the reproducibility is ± 0.1% of the full scale reading. Conversion to $CO_2(g)$ flow rates of the $O_2(g)$ controllers was made by multiplying the measured flow by the heat capacity of $O_2(g)$ at 298 K divided by the heat capacity of $CO_2(g)$ at 298 K both taken from the JANAF tables [5]. The accuracy of this conversion is ± 2% of the full scale reading. Weighings were carried out on an Ohaus GT 2100 electronic balance with a capacity of 2100 g and an accuracy of ± 0.01 g or on a Mettler Instruments semi-micro analytical balance with a capacity of 200 g and an accuracy of ± 0.00002 g.

Collection Tube Analysis

Before analysis, the outside of the silica collection tubes were wiped with a wet cloth to remove any cesium carbonate on the exterior. Each tube was then broken into three pieces, placed into a polystyrene plastic test tube, and submerged in a solution which was 10% concentrated HNO_3 and 4% concentrated HF. The plastic test tube with the dissolving sample was then placed in a sonic bath for about 2 hours. After which, it was allowed to sit in the concentrated acid solution for at least 2 days. The solution was then decanted into a 100 ml Teflon volumetric flask. The plastic test tube with the remnants of the collection tubes was filled with water and allowed to sit for at least a day. The solution was then added to the original and the volumetric flask was filled to 100 ml. The sample was then analyzed for cesium by the Inductively Coupled Plasma-Mass Spectrometry (ICP-MS) technique which is sensitive enough to detect as little as 1 nanogram of cesium and the results have an accuracy of ± 5 %.

Starting Materials

Na_2CO_3 powder of 99.97% purity was obtained from Baker Analyzed. Na_2SO_4 powder of 99.96% purity was obtained from EM Scientific. NaCl powder of 99.97% purity was obtained from EM Scientific. Cs_2CO_3 powder of 99.9% purity was obtained from Alfa Products. (Used only in experiments #10 to #20.) Cs_2CO_3 powder of 99.996% purity was obtained from Johnson Mathey Specialty Products. $CsNO_3$ powder of 99% purity was obtained from Aldrich. Spectral grade SiO_2 powder -325 mesh was obtained from the Pennsylvania Glass Sand Corporation. Pellets, roughly 1/8" in size, of molecular sieve 5A were obtained from Linde. Coal flyashes, designated as SRM 1633a and SRM 2690, were obtained from the National Institute of Standards and Technology (NIST) as standard reference materials. Compositions provided by NIST for the ashes are listed in Table 4.

Preparation and Characterization of Sample Materials

For the cesium in ash experiments, 0.40249 g of $CsNO_3$ were hand blended using a spatula with 10.57 g of SRM 2690 ash. The mixture was ground in a mortar and pestle to pass through a 200 mesh sieve and then fired at 1150°C for 19 hours in an alumina crucible. The product sintered hard. Weight losses were 0.09 g for grinding and sieving and 0.24 g for heat treatment of which 0.13 g can be attributed to nitrate decomposition. The sintered material was then crushed and ground again to pass through

Table 4. Composition of NIST standard reference material coal flyashes given in weight percent of constituent oxides.

oxide	SRM 1633a	SRM 2690
Na_2O	0.23 ± 0.01	0.32 ± 0.03
K_2O	2.26 ± 0.07	1.25 ± 0.05
MgO	0.75 ± 0.02	2.54 ± 0.08
CaO	1.55 ± 0.01	7.99 ± 0.18
SrO	0.10 ± 0.01	0.24
BaO	0.17	0.73
MnO	0.02 ± 0.01	0.04
Al_2O_3	27.02 ± 1.89	23.33 ± 0.53
Fe_2O_3	13.44 ± 0.14	5.10 ± 0.09
SiO_2	48.78 ± 1.71	55.30 ± 0.36
TiO_2	1.33	0.87 ± 0.02
SO_3	0.45	0.37 ± 0.02
P_2O_5	----	1.19 ± 0.02

Table 5. Weight percent composition of cesium in samples before and after experiments.

sample	before (wt% Cs)	after (wt% Cs)
<u>in 2690 ash</u>		
0.42wt%Cs_2O	0.40[a]	0.17[a]
<u>in Na_2CO_3</u>		
13.9wt%Cs_2CO_3	11.4[b]	8.6[a]
10.2wt%Cs_2CO_3/22.5wt%Na_2SO_4	8.3[b]	6.7[a]
12.5wt%Cs_2CO_3/10.0wt%NaCl	8.2[b]	10.0[a]
0.2wt%Cs_2CO_3	0.16[b]	0.092[a]
0.2wt%Cs_2CO_3/2.0wt%1633a ash	0.16[b]	0.090[a]

[a] based on ICP-MS chemical analysis
[b] based on weights of chemicals added

a 200 mesh sieve. Analysis of this material by the ICP-MS method showed that the ash contained 0.40wt% cesium. In the transpiration experiments, 4.9 g of this material, designated as 0.42wt%Cs_2O/2690, was placed in a platinum boat. After the transpirations experiments were completed, analysis showed that the material was 0.17wt% cesium.

For the horizontal apparatus transpiration experiments on carbonate based salts, between 4 and 12 g of Cs_2CO_3 was used for the runs on pure Cs_2CO_3, and 9.859 g of Na_2CO_3 and 1.597 g of Cs_2CO_3 was blended and used for the runs on 13.9wt%Cs_2CO_3/Na_2CO_3.

For the vertical apparatus transpiration experiments, the carbonate based samples were made by taking a spatula and hand blending the appropriate amounts of the desired materials in a round bottom alumina crucible, 5.9 cm OD by 15.3 cm high, which was then placed in the transpiration apparatus. For the runs on 13.9wt%Cs_2CO_3/Na_2CO_3, 120.00 g of Na_2CO_3 was blended with 19.42 g of Cs_2CO_3. For the runs on 10.2wt%Cs_2CO_3/22.5wt%Na_2SO_4/Na_2CO_3, 200.00 g of Na_2CO_3 was blended with 67.02 g of Na_2SO_4 and 30.30 g of Cs_2CO_3. For the runs on 12.5wt%Cs_2CO_3/10.0wt%NaCl/Na_2CO_3, 232.42 g was blended with 37.62 g of Cs_2CO_3 and 29.98 g of NaCl. For the runs on 1wt%Cs_2CO_3/10wt%1633a/Na_2CO_3, 220.00 g of Na_2CO_3 was blended with 2.001 g of Cs_2CO_3 and 22.01 g of SRM 1633a ash. For the remaining samples, about 10% of the Na_2CO_3 was retained and added to the top of the mixture after it was blended. For the experiments on 0.2wt%Cs_2CO_3/2.0wt%1633a/Na_2CO_3, 244.50 g of Na_2CO_3 was blended with 5.01 g of 1633a ash and 0.5008 g of Cs_2CO_3. For the experiments on 0.2wt%Cs_2CO_3/Na_2CO_3, 249.51 g of Na_2CO_3 was blended with 0.5002 g of Cs_2CO_3. For the experiments on 0.2wt%Cs_2CO_3/2.0wt%sieve 5A/Na_2CO_3, 244.50 g of Na_2CO_3 was blended with 5.00 g of Linde molecular sieve 5A and 0.5023 g of Cs_2CO_3. For the experiments on 0.2wt%Cs_2CO_3/ 2.0wt%SiO_2/Na_2CO_3, 244.50 g of Na_2CO_3 was blended with 5.00 g of SiO_2 and 0.5043 g of Cs_2CO_3, and for the experiments on pure Cs_2CO_3, 199.72 g of Cs_2CO_3 was used.

Weight percent compositions of cesium in some samples before and after transpiration experiments are given in Table 5. With the exception of the 0.42wt%Cs_2O/2690 ash material, the cesium compositions before the experiments were calculated from the weights of the starting materials used. After the transpiration experiments, the cesium compositions were obtained by ICP-MS analysis. With the exception of the

10.2wt%Cs_2CO_3/22.5wt%Na_2SO_4/Na_2CO_3 sample, a decrease in cesium composition after the transpiration experiments was observed.

Analysis of Results

The experiments conducted on the 0.42wt%Cs_2O/2690 ash material using the horizontal apparatus are summarized in Tables 6 and 7. With finely divided solid present, the horizontal apparatus is expected to provide good equilibrium measurements. The experiments conducted on the molten carbonate based systems are summarized in Tables 8 and 9. Both the horizontal and vertical apparatuses were used for these experiments. The vertical apparatus is expected to more readily achieve equilibrium results since the carrier gas is bubbled through the melt which results in a high contact area. However, the horizontal apparatus was available from previous work on uranium oxide volatility [14], and experiments were conducted on the apparatus to obtain additional information.

Water Vapor Effect

The effect of leaving out water vapor was tested a number of times. With the exception of the experiments on 12.5wt%Cs_2CO_3/10.0wt%NaCl/Na_2CO_3, the data show that the cesium volatility is reduced at least an order of magnitude when $H_2O(g)$ is absent. This verifies that CsOH(g) is the major vapor species when $H_2O(g)$ is present, as expected. When 10.0wt% NaCl was present in the sample, CsCl(g) became the dominant species and as expected $H_2O(g)$ has no effect on the vapor pressure of CsCl(g).

Horizontal versus Vertical Configuration

Two molten carbonate compositions were studied on both apparatuses, pure Cs_2CO_3 and 13.9wt%Cs_2CO_3/Na_2CO_3. For pure Cs_2CO_3, the volatility measurements from both apparatuses are compared in Figure 5. The consistency of the data from the vertical apparatus is excellent whereas the consistency of the data from the horizontal apparatus is poor. With the exception of the data at 1173 K and one data point at 1223 K, the vapor pressure data from the horizontal furnace lies between a factor of 3 and 40 lower than in the vertical apparatus. For 13.9wt%Cs_2CO_3/Na_2CO_3, the volatility measurements from both apparatuses are compared in Figure 6. Both sets of data show good consistency. With one exception, the vapor pressure data from the horizontal furnace is about a factor of 3 lower than

Table 6. Summary of transpiration experiments for experiments on $Cs_2O(s)$ interacted with ash.

run #	sample	T_{furn} (K)	O_2 flow (cm^3/min)	time (min)	T_{bath} (°C)	H_2O (g)	apparatus
1	0.42%Cs_2O/2690	1173	25.0	1635			horiz
2	0.42%Cs_2O/2690	1173	20.0	1880	85.5	32.5	horiz
3	0.42%Cs_2O/2690	1173	20.0	1320	85.5	30.92	horiz
4	0.42%Cs_2O/2690	1073	15.0	1875	86	36.83	horiz
5	0.42%Cs_2O/2690	1073	25.0	3375			horiz
6	0.42%Cs_2O/2690	1273	25.0	492			horiz
7	0.42%Cs_2O/2690	1273	20.0	465	82	8.68	horiz
8	0.42%Cs_2O/2690	1173	20.0	485	76	4.93	horiz
9	0.42%Cs_2O/2690	1173	15.0	505	90	13.39	horiz

Table 7. Summary of transpiration experiments for experiments on $Cs_2O(s)$ interacted with ash.

run	moles of gas			$p(O_2)$	$p(H_2O)$	Cs	p(Cs total)
#	O_2	H_2O	total	(atm)	(atm)	(ng)	(atm)
1	1.8236		1.8236	1.000		7375	3.043×10^{-8}
2	1.6775	1.8029	3.4804	0.4820	0.5180	630	1.362×10^{-9}
3	1.1778	1.7163	2.8941	0.4070	0.5930	303	7.877×10^{-10}
4	1.2548	2.0444	3.2992	0.3803	0.6197	89	2.030×10^{-10}
5	3.7644		3.7644	1.000		121	2.418×10^{-10}
6	0.5488		0.5488	1.000		885	1.213×10^{-8}
7	0.4149	0.4818	0.8967	0.4627	0.5373	1073	9.004×10^{-9}
8	0.4328	0.2737	0.7065	0.6126	0.3874	89	9.478×10^{-10}
9	0.3380	0.7433	1.0813	0.3126	0.6874	98	6.819×10^{-10}

Table 8. Summary of transpiration experiments for experiments on molten carbonates.

run #	sample	T_{furn} (K)	gas flow (cm^3/min)	time (min)	T_{bath} (°C)	H_2O (g)	apparatus
10	Cs_2CO_3	1124.2	25.6	180	76.7	1.81	horiz
11	Cs_2CO_3	1124.2	25.5	180	75.1	3.81	horiz
12	Cs_2CO_3	1122.4	25.5	180	76.3	3.43	horiz
13	Cs_2CO_3	1124.2	76.3	90	74.4	3.57	horiz
14	13.9%Cs_2CO_3	1220.2	76.3	120	75.0	2.54	vert
15	13.9%Cs_2CO_3	1231.7	76.3	120	75.1	2.84	vert
16	13.9%Cs_2CO_3	1225.8	76.3	180			vert
17	13.9%Cs_2CO_3	1226.8	76.3	120	75.4	3.69	vert
18	13.9%Cs_2CO_3	1224.7	25.5	120	95.2	8.30	vert
19	13.9%Cs_2CO_3	1124.4	25.5	120	95.1	9.56	vert
20	13.9%Cs_2CO_3	1176.0	25.5	120	89.9	4.98	vert
21	10.2%Cs_2CO_3/22.5%Na_2SO_4	1175.6	25.5	185	90.0	6.11	vert
22	10.2%Cs_2CO_3/22.5%Na_2SO_4	1124.5	25.5	180	94.6	19.33	vert
23	10.2%Cs_2CO_3/22.5%Na_2SO_4	1125.4	76.4	180	74.8	6.66	vert
24	10.2%Cs_2CO_3/22.5%Na_2SO_4	1125.5	76.3	180			vert
25	10.2%Cs_2CO_3/22.5%Na_2SO_4	1126.5	76.3	180	75.5	5.88	vert
26	10.2%Cs_2CO_3/22.5%Na_2SO_4	1124.0	76.3	180			horiz
27	10.2%Cs_2CO_3/22.5%Na_2SO_4	1225.7	25.5	180	94.6	13.98	vert
28	13.9%Cs_2CO_3	1224.5	76.3	180	75.7	7.16	horiz
29	10.2%Cs_2CO_3/22.5%Na_2SO_4	1177.4	76.3	180	75.4	5.57	vert
30	13.9%Cs_2CO_3	1223.4	51.0	180	94.6	44.78	horiz
31	13.9%Cs_2CO_3	1123.1	51.0	180	94.7	47.79	horiz
32	13.9%Cs_2CO_3	1123.6	76.3	180	74.9	6.85	horiz
33	13.9%Cs_2CO_3	1126.0	76.3	240			horiz
34	13.9%Cs_2CO_3	1223.0	76.3	180	74.8	6.66	horiz
35	13.9%Cs_2CO_3	1174.8	76.3	180	75.2	6.30	horiz
36	12.5%Cs_2CO_3/10%NaCl	1127.9	76.3	180			vert
37	12.5%Cs_2CO_3/10%NaCl	1127.0	76.3	180	75.3	5.67	vert
38	Cs_2CO_3	1124.6	76.3	180			horiz
39	12.5%Cs_2CO_3/10%NaCl	1082.4	51.0	180			vert
40	Cs_2CO_3	1224.4	51.0	180			horiz
41	12.5%Cs_2CO_3/10%NaCl	1075.1	25.5	180	94.8	16.26	vert
42	Cs_2CO_3	1223.8	20.3	180	75.6	1.73	horiz
43	12.5%Cs_2CO_3/10%NaCl	1183.1	10.2	180	94.9	4.47	vert
44	Cs_2CO_3	1225.6	10.2	180	94.9	6.04	horiz
45	12.5%Cs_2CO_3/10%NaCl	1226.0	10.2	180	74.6	1.27	vert
46	1%Cs_2CO_3/10%1633a	1173	25.5	180			vert
49	1%Cs_2CO_3/10%1633a	1235.0	25.5	240	94.4	()	vert
50	0.2%Cs_2CO_3/2%1633a	1173	25.6	180			vert
51	0.2%Cs_2CO_3/2%1633a	1226.3	25.5	240	95.1	20.44	vert
52	0.2%Cs_2CO_3/2%1633a	1127.2	25.5	240	94.8	21.21	vert
53	0.2%Cs_2CO_3/2%1633a	1123.3	76.3	240	75.0	9.67	vert
54	0.2%Cs_2CO_3/2%1633a	1173.8	76.3	245	74.7	7.45	vert
55	0.2%Cs_2CO_3/2%1633a	1174.0	25.5	240	94.8	21.71	vert

Table 8. (cont.) Summary of transpiration experiments for experiments on molten carbonates.

run #	sample	T_{furn} (K)	gas flow (cm^3/min)	time (min)	T_{bath} (°C)	H_2O (g)	apparatus
56	0.2%Cs_2CO_3/2%1633a	1221.1	50.9	240	75.2	5.28	vert
57	0.2%Cs_2CO_3	1139	51.0	216		0.86	vert
58	0.2%Cs_2CO_3	1173.3	76.3	240	75.2	7.35	vert
59	Cs_2CO_3	1174.3	50.9	120	75.3	3.22	horiz
60	0.2%Cs_2CO_3	1173.8	25.5	180	94.9	16.46	vert
61	Cs_2CO_3	1175.6	25.5	120	94.8	16.43	horiz
62	0.2%Cs_2CO_3	1221.5	76.3	180	74.7	7.67	vert
63	Cs_2CO_3	1223.3	51.0	120	75.5	3.54	horiz
64	0.2%Cs_2CO_3	1221.6	25.5	180	95.0	14.46	vert
65	Cs_2CO_3	1225.2	25.5	120	94.1	12.62	horiz
66	0.2%Cs_2CO_3	1272.1	76.3	180	74.9	7.38	vert
67	Cs_2CO_3	1273.3	76.3	120	75.2	5.03	horiz
68	Cs_2CO_3	1072.1	25.5	180	94.8	21.49	horiz
69	0.2%Cs_2CO_3/2%sieve 5A	1173	76.3	155			vert
70	0.2%Cs_2CO_3/2%sieve 5A	1173.4	25.5	240	94.8	12.56	vert
71	Cs_2CO_3	1073.5	76.3	120	75.5	5.07	horiz
72	0.2%Cs_2CO_3/2%sieve 5A	1173.4	76.3	180	75.1	7.72	vert
73	Cs_2CO_3	1174.3	76.3	170			horiz
74	0.2%Cs_2CO_3/2%sieve 5A	1225.3	76.3	180	74.9	5.47	vert
75	Cs_2CO_3	1176.2	76.3	180			horiz
76	0.2%Cs_2CO_3/2%sieve 5A	1226.2	25.5	180	95.0	16.58	vert
77	Cs_2CO_3	1173.9	76.3	180	75.0	6.52	horiz
80	0.2%Cs_2CO_3/2%sieve 5A	1273.7	51.0	180	75.2	3.72	vert
81	Cs_2CO_3	1174.6	51.0	180	76.2	6.13	horiz
82	Cs_2CO_3	1172.6	25.5	180	75.6	2.28	horiz
83	Cs_2CO_3	1176.6	15.3	180	74.8	1.15	horiz
84	0.2%Cs_2CO_3/2%SiO_2	1173	25.5	120			horiz
85	0.2%Cs_2CO_3/2%SiO_2	1174.2	51.0	240			vert
86	Cs_2CO_3	1174.2	10.2	180	76.2	0.84	horiz
87	0.2%Cs_2CO_3/2%SiO_2	1173.7	25.5	180	94.7	14.25	vert
88	Cs_2CO_3	1173.3	5.3	180	75.3	0.31	horiz
89	0.2%Cs_2CO_3/2%SiO_2	1173	25.6	180			vert
90	0.2%Cs_2CO_3/2%SiO_2	1173.5	25.5	180	95.3	17.73	vert
91	0.2%Cs_2CO_3/2%SiO_2	1174.4	76.3	180	74.5	6.18	vert
92	0.2%Cs_2CO_3/2%SiO_2	1224.5	76.3	180	75.1	5.99	vert
93	0.2%Cs_2CO_3/2%SiO_2	1221.9	25.5	180	95.1	16.29	vert
94	Cs_2CO_3	1173	49.0	210			vert
95	Cs_2CO_3	1124.3	76.3	180	75.1	3.41	vert
96	Cs_2CO_3	1120.4	25.5	180	95.0	4.61	vert
97	Cs_2CO_3	1172.0	76.3	180	75.1	3.23	vert
98	Cs_2CO_3	1169.6	25.5	180	94.7	5.00	vert
99	Cs_2CO_3	1220.9	76.3	180	74.5	2.92	vert
100	Cs_2CO_3	1269.2	76.3	182	75.2	2.83	vert

Table 9. Summary of transpiration experiments for experiments on molten carbonates.

run	moles of gas			$p(CO_2)$	$p(H_2O)$	Cs	p(Cs total)
#	CO_2	H_2O	total	(atm)	(atm)	(mg)	(atm)
10	0.2052	0.1005	0.3057	0.6712	0.3288	0.94	2.314×10^{-5}
11	0.2046	0.2115	0.4161	0.4917	0.5083	7.70	1.392×10^{-4}
12	0.2046	0.1904	0.3950	0.5180	0.4820	8.90	1.695×10^{-4}
13	0.3066	0.1982	0.5048	0.6074	0.3926	10.91	1.626×10^{-4}
14	0.4088	0.1410	0.5498	0.7435	0.2565	12.02	1.645×10^{-4}
15	0.4088	0.1576	0.5664	0.7218	0.2782	11.74	1.560×10^{-4}
16	0.6131		0.6131	1.000		1.32	1.620×10^{-5}
17	0.4088	0.2048	0.6136	0.6662	0.3338	16.06	1.969×10^{-4}
18	0.1364	0.4607	0.5971	0.2284	0.7716	40.69	5.127×10^{-4}
19	0.1364	0.5307	0.6671	0.2045	0.7955	7.606	8.579×10^{-5}
20	0.1364	0.2764	0.4128	0.3304	0.6696	8.264	1.506×10^{-4}
21	0.2103	0.3392	0.5495	0.3827	0.6173	9.26	1.268×10^{-4}
22	0.2046	1.0730	1.2776	0.1601	0.8399	8.93	5.259×10^{-5}
23	0.6133	0.3697	0.9830	0.6239	0.3761	1.88	1.439×10^{-5}
24	0.6131		0.6131	1.000		0.11	1.350×10^{-6}
25	0.6131	0.3264	0.9395	0.6526	0.3474	11.47	9.186×10^{-5}
26	0.6131		0.6131	1.000		1.89	2.320×10^{-5}
27	0.2046	0.7760	0.9806	0.2086	0.7914	29.30	2.248×10^{-4}
28	0.6131	0.3974	1.0105	0.6067	0.3933	29.41	2.190×10^{-4}
29	0.6131	0.3092	0.9223	0.6648	0.3352	4.57	3.728×10^{-5}
30	0.4092	2.4857	2.8949	0.1414	0.8586	87.94	2.286×10^{-4}
31	0.4092	2.6528	3.0620	0.1336	0.8664	10.84	2.664×10^{-5}
32	0.6131	0.3802	0.9933	0.6172	0.3828	1.67	1.265×10^{-5}
33	0.8175		0.8175	1.000		0.03	2.761×10^{-7}
34	0.6131	0.3697	0.9828	0.6238	0.3762	9.68	7.411×10^{-5}
35	0.6131	0.3497	0.9628	0.6368	0.3632	3.16	2.470×10^{-5}
36	0.6131		0.6131	1.000		39.47	4.844×10^{-4}
37	0.6131	0.3147	0.9278	0.6608	0.3392	65.25	5.292×10^{-4}
38	0.6131		0.6131	1.000		1.24	1.522×10^{-5}
39	0.4092		0.4092	1.000		20.09	3.694×10^{-4}
40	0.4092		0.4092	1.000		5.74	1.055×10^{-4}
41	0.2046	0.9026	1.1072	0.1848	0.8152	56.35	3.829×10^{-4}
42	0.1633	0.0960	0.2593	0.6298	0.3702	72.70	2.110×10^{-3}
43	0.0820	0.2481	0.3301	0.2484	0.7516	44.01	1.003×10^{-3}
44	0.0820	0.3353	0.4173	0.1965	0.8035	148.7	2.681×10^{-3}
45	0.0820	0.0705	0.1525	0.5377	0.4623	33.06	1.631×10^{-3}
48	0.8175		0.8175	1.000		0.437	4.022×10^{-6}
49	0.2728		0.2728	1.000		3.15	8.688×10^{-5}
50	0.2059		0.2059	1.000		0.084	3.070×10^{-6}
51	0.2728	1.1346	1.4074	0.1938	0.8062	1.00	5.346×10^{-6}
52	0.2728	1.1773	1.4501	0.1881	0.8119	0.842	4.369×10^{-6}
53	0.8175	0.5368	1.3543	0.6036	0.3964	0.324	1.800×10^{-6}
54	0.8346	0.4135	1.2481	0.6687	0.3313	0.333	2.008×10^{-6}
55	0.2728	1.2051	1.4779	0.1846	0.8154	0.905	4.608×10^{-6}

Table 9. (cont.) Summary of transpiration experiments for experiments on molten carbonates.

run	moles of gas			$p(CO_2)$	$p(H_2O)$	Cs	p(Cs total)
#	CO_2	H_2O	total	(atm)	(atm)	(mg)	(atm)
56	0.5447	0.2931	0.8378	0.6502	0.3498	0.426	$3.826x10^{-6}$
57	0.4910	0.0477	0.5387	0.9115	0.0885	0.166	$2.318x10^{-6}$
58	0.8175	0.4080	1.2255	0.6671	0.3329	0.279	$1.713x10^{-6}$
59	0.2724	0.1787	0.4511	0.6039	0.3961	89.9	$1.500x10^{-3}$
60	0.2046	0.9137	1.1183	0.1830	0.8170	0.472	$3.176x10^{-6}$
61	0.1364	0.9120	1.0484	0.1301	0.8699	286.2	$2.054x10^{-3}$
62	0.6131	0.4258	1.0389	0.5901	0.4099	0.818	$5.924x10^{-6}$
63	0.2728	0.1965	0.4693	0.5813	0.4187	54.4	$8.722x10^{-4}$
64	0.2046	0.8027	1.0073	0.2031	0.7969	0.969	$7.238x10^{-6}$
65	0.1364	0.7005	0.8369	0.1631	0.8370	23.5	$2.113x10^{-4}$
66	0.6131	0.4097	1.0228	0.5994	0.4006	0.801	$5.892x10^{-6}$
67	0.4088	0.2792	0.6880	0.5942	0.4058	23.5	$2.570x10^{-4}$
68	0.2046	1.1929	1.3975	0.1464	0.8536	2.09	$1.125x10^{-5}$
69	0.5280		0.5280	1.000		0.126	$1.796x10^{-6}$
70	0.2728	0.6972	0.9700	0.2812	0.7188	1.39	$1.078x10^{-5}$
71	0.4088	0.2814	0.6902	0.5923	0.4077	0.661	$7.206x10^{-6}$
72	0.6131	0.4285	1.0416	0.5886	0.4114	0.611	$4.414x10^{-6}$
73	0.5791		0.5791	1.000		36.9	$4.794x10^{-4}$
74	0.6131	0.3036	0.9167	0.6688	0.3312	0.348	$2.856x10^{-6}$
75	0.6131		0.6131	1.000		55.5	$6.811x10^{-4}$
76	0.2046	0.9203	1.1249	0.1819	0.8181	0.790	$5.284x10^{-6}$
77	0.6131	0.3619	0.9750	0.6288	0.3712	196	$1.512x10^{-3}$
80	0.4092	0.2065	0.6157	0.6646	0.3354	0.184	$2.248x10^{-6}$
81	0.4092	0.3403	0.7495	0.5460	0.4540	106	$1.064x10^{-3}$
82	0.2046	0.1266	0.3312	0.6178	0.3822	41.1	$9.337x10^{-4}$
83	0.1226	0.0638	0.1864	0.6577	0.3423	27.4	$1.106x10^{-3}$
84	0.1364		0.1364	1.000		0.050	$2.758x10^{-6}$
85	0.5456		0.5456	1.000		0.051	$7.033x10^{-7}$
86	0.0820	0.0466	0.1286	0.6376	0.3624	13.4	$7.840x10^{-4}$
87	0.2046	0.7910	0.9956	0.2055	0.7945	0.462	$3.492x10^{-6}$
88	0.0427	0.0172	0.0599	0.7129	0.2871	19.2	$2.412x10^{-3}$
89	0.2052		0.2052	1.000		0.075	$2.750x10^{-6}$
90	0.2046	0.9842	1.1888	0.1721	0.8279	0.770	$4.874x10^{-6}$
91	0.6131	0.3430	0.9561	0.6413	0.3587	0.264	$2.078x10^{-6}$
92	0.6131	0.3325	0.9456	0.6484	0.3516	0.433	$3.445x10^{-6}$
93	0.2046	0.9042	1.1088	0.1845	0.8155	1.82	$1.235x10^{-5}$
94	0.4588		0.4588	1.000		27	$4.428x10^{-4}$
95	0.6131	0.1893	0.8024	0.7641	0.2359	46	$4.313x10^{-4}$
96	0.2046	0.2559	0.4605	0.4443	0.5557	63	$1.029x10^{-3}$
97	0.6131	0.1793	0.7924	0.7737	0.2263	113	$1.073x10^{-3}$
98	0.2046	0.2775	0.4821	0.4244	0.5756	131	$2.044x10^{-3}$
99	0.6131	0.1621	0.7752	0.7909	0.2091	222	$2.155x10^{-3}$
100	0.6200	0.1571	0.7771	0.7978	0.2022	439	$4.250x10^{-3}$

from the vertical apparatus, the exception shows agreement between both apparatuses. At 1173 K, a flow rate test was conducted on the horizontal unit. A plot of flow rate versus the equilibrium constant for the generation of CsOH(g) from Cs_2CO_3(l) is given in Figure 7. At flow rates below about 10 cm^3/min, the data indicate that gaseous diffusion is a problem. However, higher flow rates seem to give good data. These data all fall at or near the data measured on the vertical unit. Although the horizontal unit clearly yields less accurate measurements than the vertical, the data obtained from it can still be used to support conclusions that follow.

Concentration Effect

The effect of cesium concentration on cesium volatility was obtained by comparing cesium volatility measurements from 13.9wt%Cs_2CO_3/Na_2CO_3 and 0.2wt%Cs_2CO_3/Na_2CO_3 with measurements from pure Cs_2CO_3. A plot of the logarithm of the equilibrium constant for the generation of CsOH(g) given by eqn (10) versus reciprocal temperature is given in Figure 8. Each set of data shows good linearity with matching slopes, indicating good consistency and reproducability. The data on 13.9wt%Cs_2CO_3/Na_2CO_3 and 0.2wt%Cs_2CO_3/Na_2CO_3 are reduced approximately by their mole fractions of cesium carbonate, i.e. by a factor of 0.0500 and 0.000652, respectively. Thus, Raoult's law seems to be observed.

Sulfate Effect

The effect of sulfate on cesium volatility was obtained by comparing cesium volatility measurements from 10.2wt%Cs_2CO_3/22.5wt%Na_2SO_4/Na_2CO_3 with measurements from 13.9wt%Cs_2CO_3/Na_2CO_3. A plot of the logarithm of the equilibrium constant for the generation of CsOH(g) given by eqn (10) versus reciprocal temperature is given in Figure 9. With two exceptions, both of which are assumed to be spurious, the sulfate mixture shows a lower volatility than the carbonate only mixture. The reduction in volatility due to the presence of about 20wt% sulfate is just under a factor of 2. The same reduction in volatility is assumed to occur at lower concentrations of cesium in the carbonate based mixture.

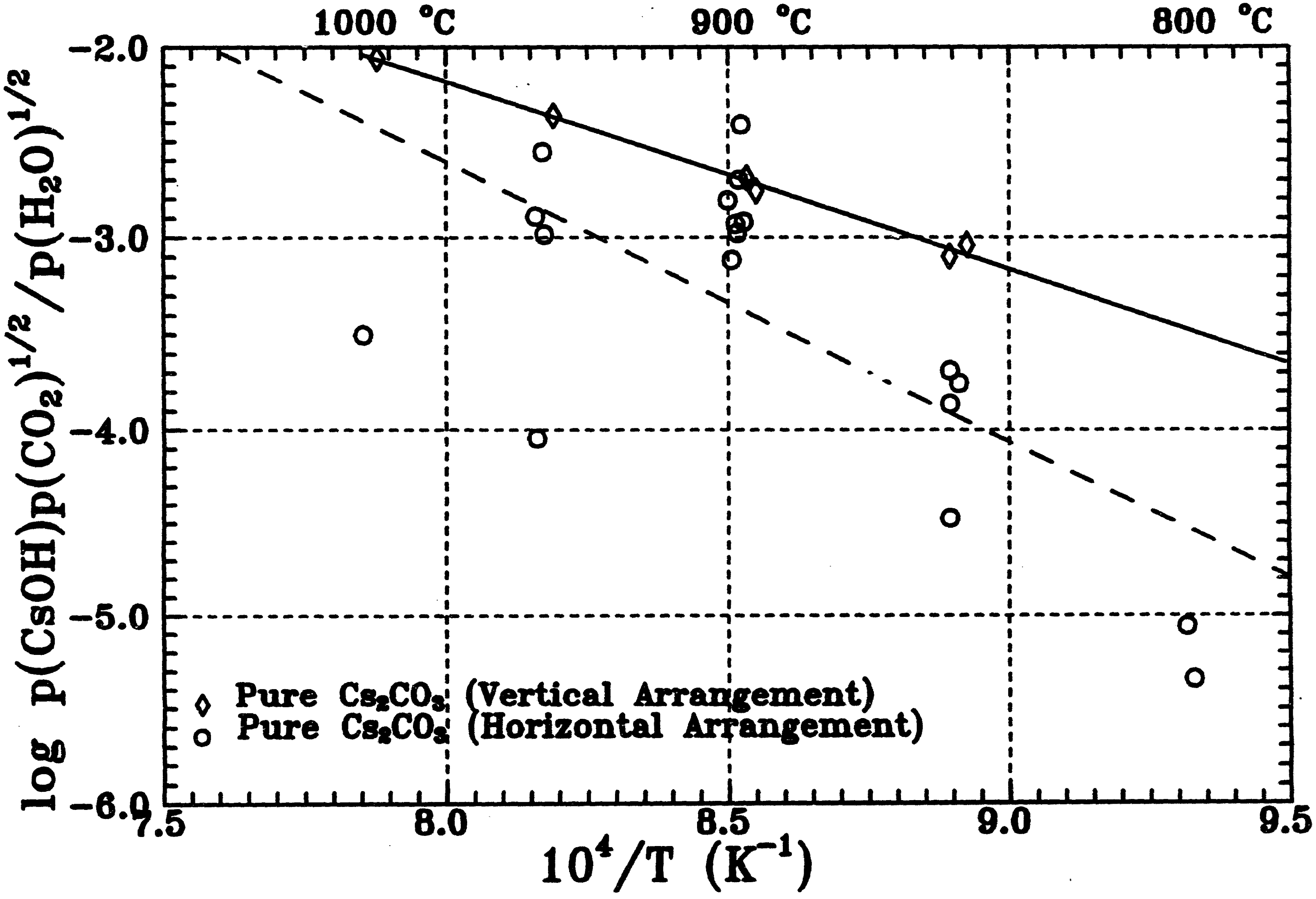

Figure 5. Plot showing log $p(CsOH)p(CO_2)^{1/2}/p(H_2O)^{1/2}$ as a function of $10^4/T$ for experiments on pure Cs_2CO_3 conducted in the horizontal and vertical apparatuses.

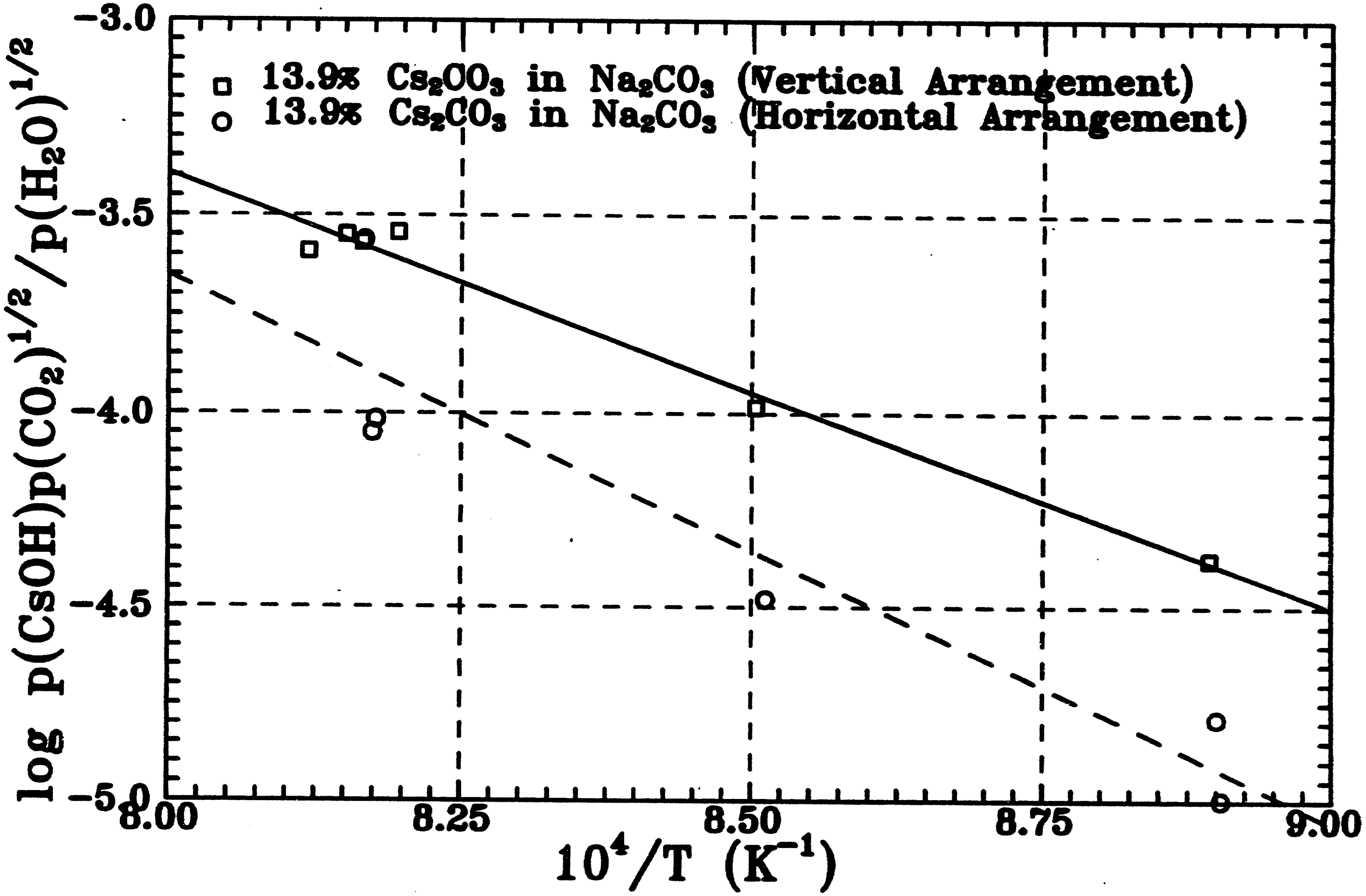

Figure 6. Plot showing log $p(CsOH)p(CO_2)^{1/2}/p(H_2O)^{1/2}$ as a function of $10^4/T$ for experiments on 13.9wt%Cs_2CO_3/Na_2CO_3 conducted in the horizontal and vertical apparatuses.

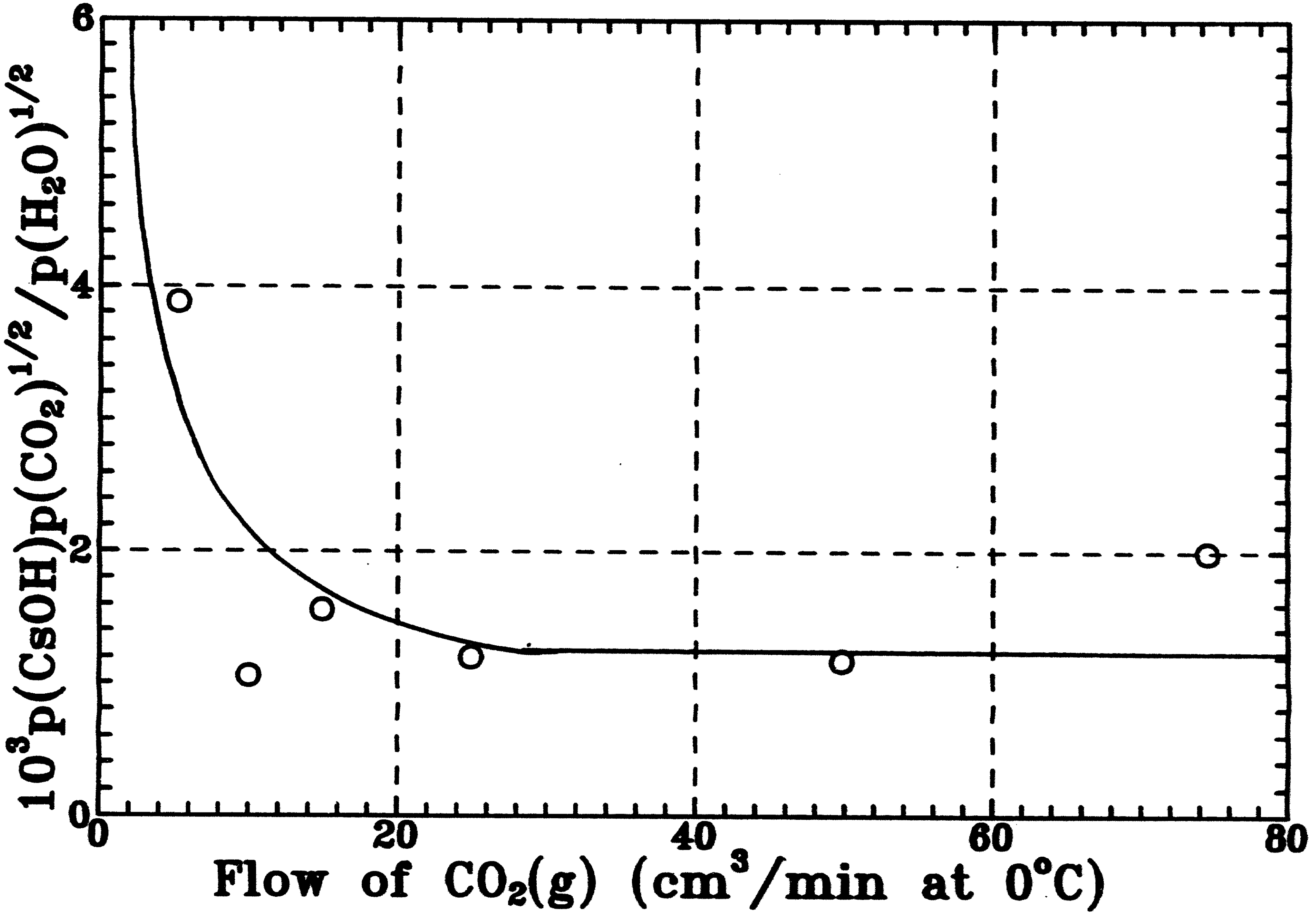

Figure 7. Plot showing $[p(CsOH)p(CO_2)^{1/2}/p(H_2O)^{1/2}]\times10^3$ as a function of CO_2(g) flow rate for experiments on pure Cs_2CO_3 conducted on the horizontal apparatus at 1173 K.

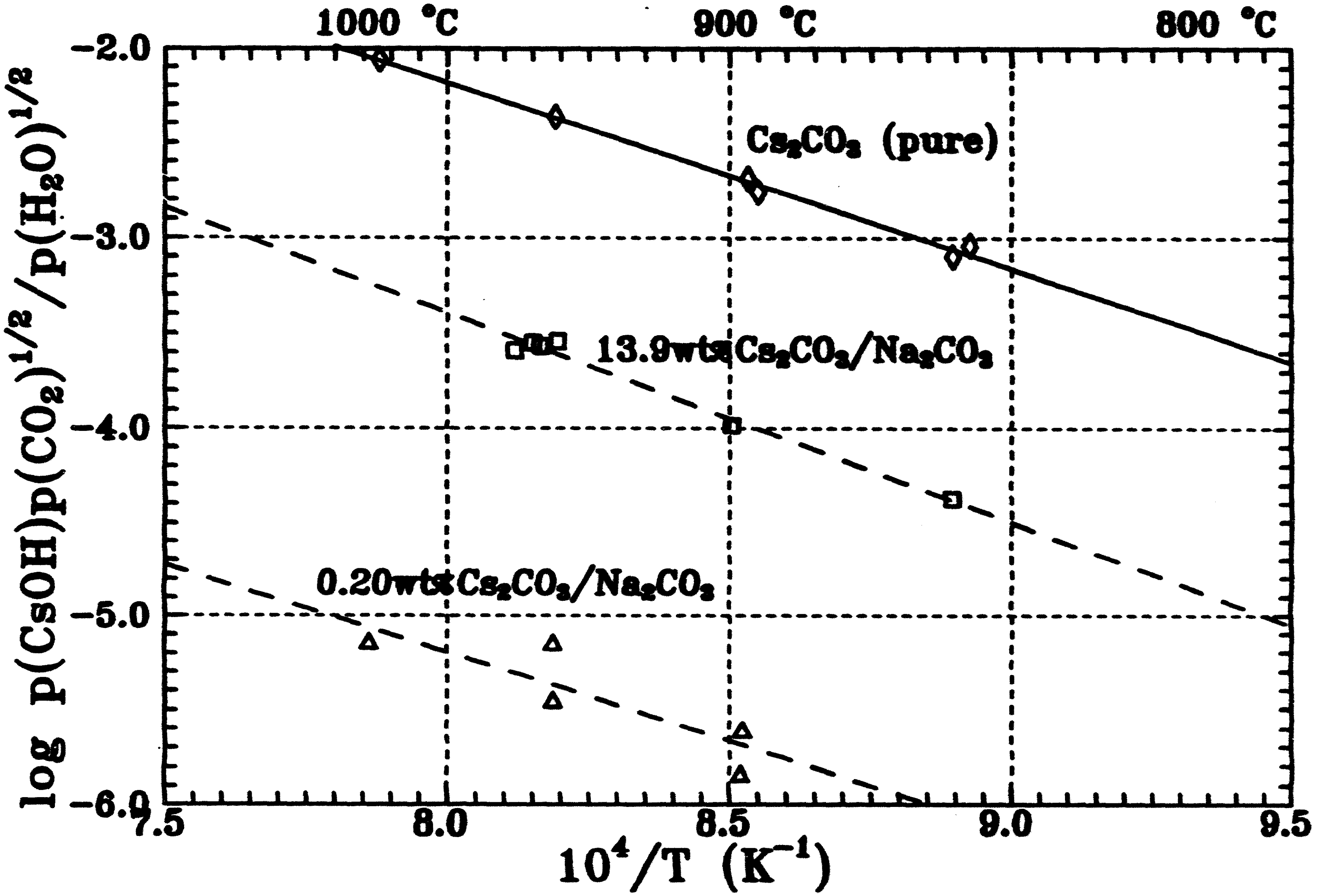

Figure 8. Plot showing log $p(CsOH)p(CO_2)^{1/2}/p(H_2O)^{1/2}$ as a function of $10^4/T$ for experiments on pure Cs_2CO_3, 13.9wt%Cs_2CO_3/Na_2CO_3, and 0.2wt%Cs_2CO_3/Na_2CO_3 conducted on the vertical apparatus.

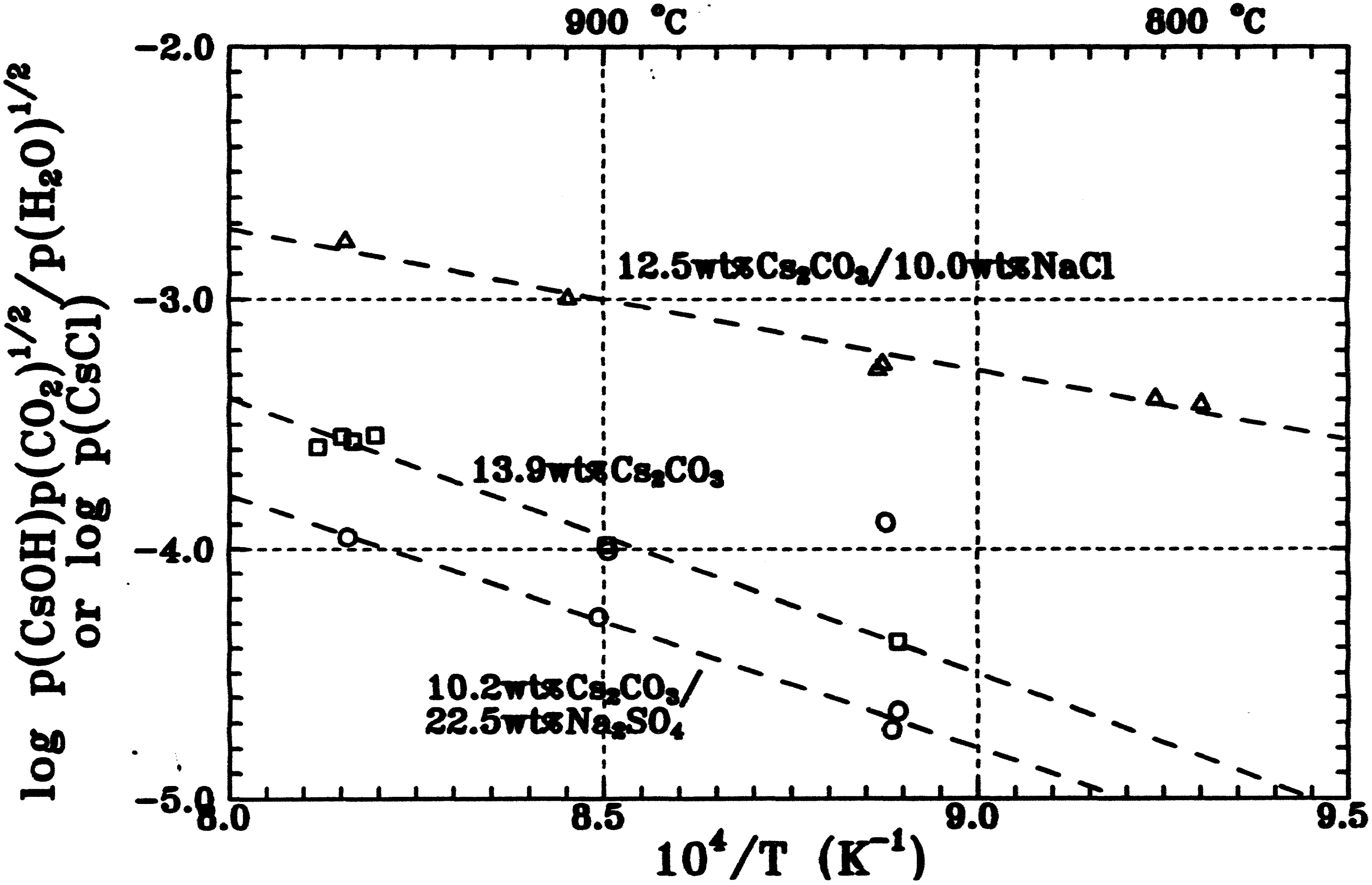

Figure 9. Plot showing log $p(CsOH)p(CO_2)^{1/2}/p(H_2O)^{1/2}$ as a function of $10^4/T$ for experiments on 13.9wt%Cs_2CO_3/Na_2CO_3 and 10.2wt%Cs_2CO_3/ 22.5wt%Na_2SO_4/Na_2CO_3 and log p(CsCl) as a function of $10^4/T$ for experiments on 12.5wt%Cs_2CO_3/10.0wt%NaCl/Na_2CO_3 conducted on the vertical apparatus.

Chloride Effect

The effect of chloride on cesium volatility was obtained by comparing cesium volatility measurements from 12.5wt%Cs_2CO_3/10.0wt%NaCl/Na_2CO_3 with measurements from 13.9wt%Cs_2CO_3/Na_2CO_3. The data are also compared in Figure 9. The volatility data are not affected by the $H_2O(g)$ pressure which implies, as expected, that CsCl(g) is the major vapor species. In Figure 9, the equilibrium constants for the generation of CsOH(g) above 13.9wt%Cs_2CO_3/Na_2CO_3 are plotted as a function of reciprocal temperature and the logarithm of the equilibrium constants for the generation of CsCl(g) above 12.5wt%Cs_2CO_3/10.0wt%NaCl/Na_2CO_3 given by eqn (11) are plotted as a function of reciprocal temperature. The addition of the chloride increases the cesium volatility dramatically, about an order of magnitude at 1200 K. The same increase in volatility from CsCl(g) is assumed to occur at lower concentrations of cesium in carbonate-chloride mixtures.

Ash Effect

The effect of ash on cesium volatility was obtained by comparing volatility measurements from 0.42wt%Cs_2O/2690, 0.2wt%Cs_2CO_3/2.0wt%1633a/Na_2CO_3, 0.2wt%Cs_2CO_3/2.0wt%sieve5A/Na_2CO_3, and 0.2wt%Cs_2CO_3/2.0wt%SiO_2/Na_2CO_3 with measurements from 0.2wt%Cs_2CO_3/Na_2CO_3. The data for the carbonate based systems are compared in Figure 10. Within the experimental error, 2.0 wt% of 1633a ash, molecular sieve 5A, or silica seem to have no effect on cesium volatility. However, the data for the molecular sieve seem to show a trend with time. In these experiments, the low-temperature runs were completed first and the high-temperature runs were completed last. The low-temperature runs lie above the curve given by 0.2wt%Cs_2CO_3/Na_2CO_3 and the high-temperature runs lie at or below the curve given by 0.2wt%Cs_2CO_3/Na_2CO_3. This suggests that some interaction may occur at higher temperatures over a period of time, thus resulting in a lowered cesium volatility.

The data for 0.42wt%Cs_2O/2690, 0.2wt%Cs_2CO_3/Na_2CO_3, and 0.2wt%Cs_2CO_3/2.0wt%1633a/Na_2CO_3 are compared in Figure 11. The volatility data for 0.42wt%Cs_2O/2690 lie about 3 orders of magnitude below the volatility data for 0.2wt%Cs_2CO_3/Na_2CO_3 and 0.2wt%Cs_2CO_3/2.0wt%1633a/Na_2CO_3. Although no reduction in cesium volatility occurs for the 2wt% ash mixture, this data suggests that higher concentrations of ash in the carbonate melt could show a significant decrease in cesium

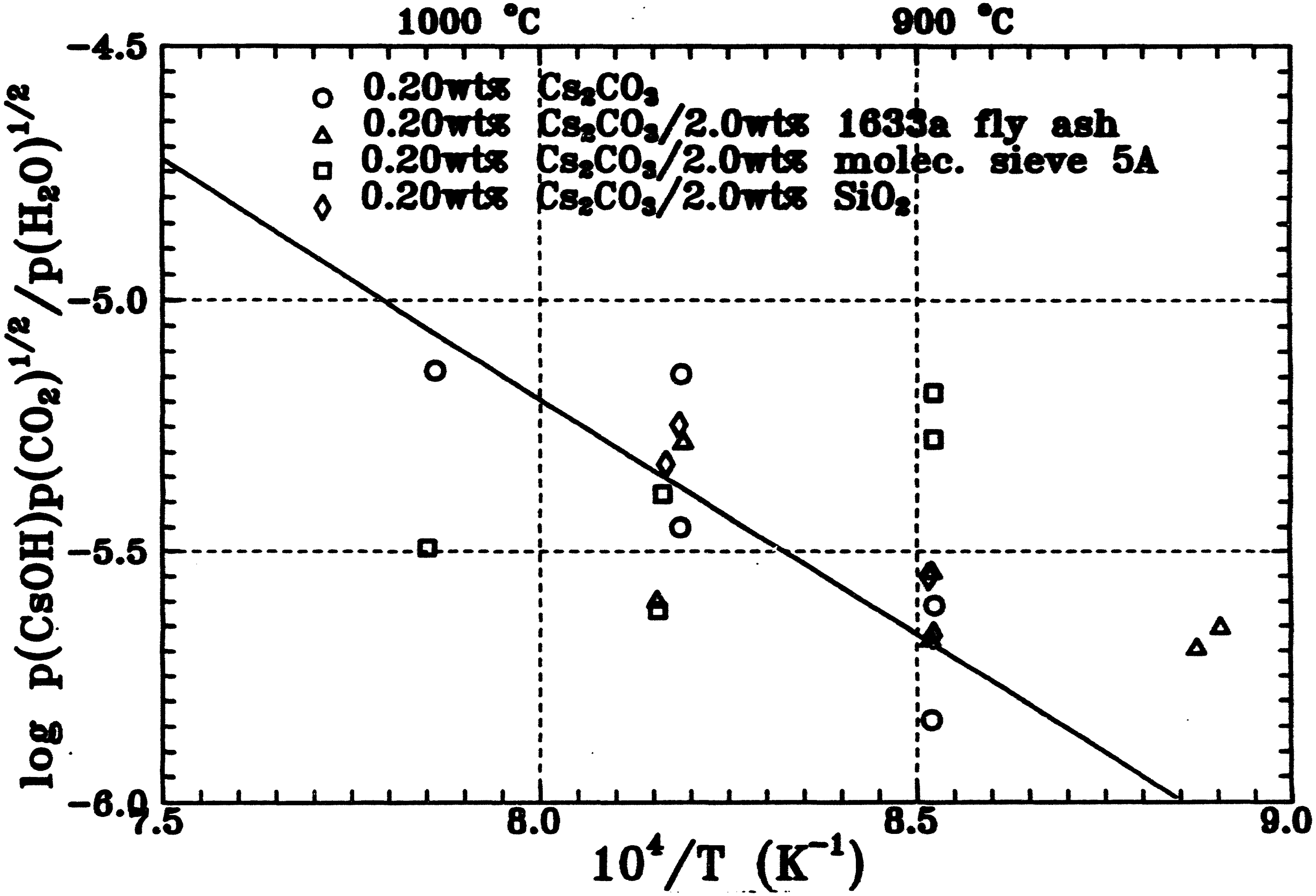

Figure 10. Plot showing log $p(CsOH)p(CO_2)^{1/2}/p(H_2O)^{1/2}$ as a function of $10^4/T$ for experiments on $0.2wt\%Cs_2CO_3/Na_2CO_3$, $0.2wt\%Cs_2CO_3/2.0wt\%1633a/Na_2CO_3$, $0.2wt\%Cs_2CO_3/2.0wt\%Sieve5A/Na_2CO_3$, and $0.2wt\%Cs_2CO_3/2.0wt\%SiO_2/Na_2CO_3$ conducted on the vertical apparatus.

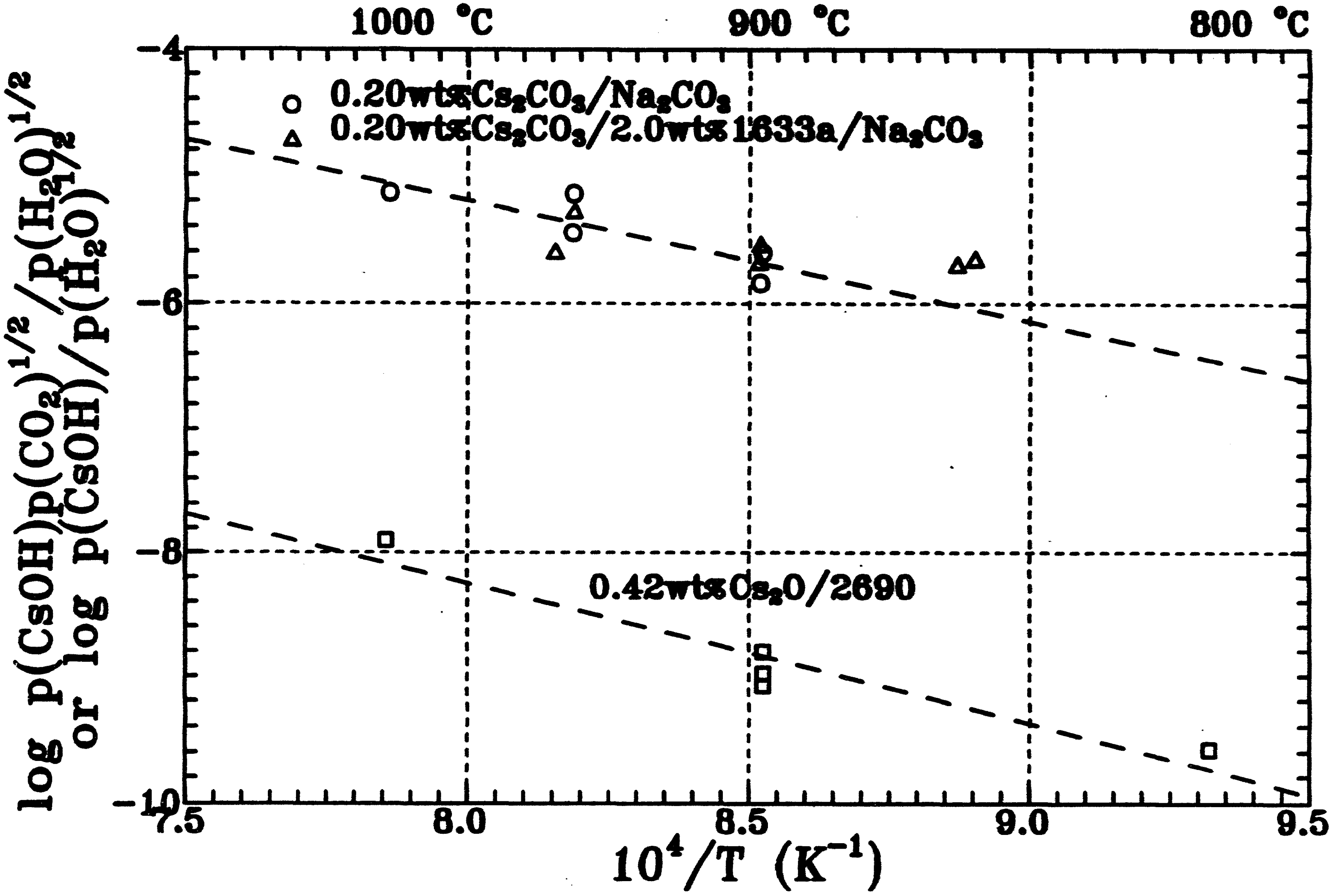

Figure 11. Plot showing log $p(CsOH)p(CO_2)^{1/2}/p(H_2O)^{1/2}$ as a function of $10^4/T$ for experiments on 0.2wt%Cs_2CO_3/Na_2CO_3 and 0.2wt%Cs_2CO_3/2.0wt%1633a/Na_2CO_3 conducted on the vertical apparatus and log $p(CsOH)/p(H_2O)^{1/2}$ as a function of $10^4/T$ for experiments on 0.42wt%Cs_2O/2690 conducted on the horizontal apparatus.

volatility. At only 2wt%, the ash is probably completely dissolved in the carbonate melt and is thus ineffective in forming solid oxides with cesium.

Thermodynamic Parameters

Standard Entropy of $Cs_2CO_3(s)$:

The standard entropy of $Cs_2CO_3(s)$ can be derived from the measured equilibrium constants for reaction (10) using pure Cs_2CO_3 in the vertical apparatus. The data taken in the horizontal apparatus are not used because of the large scatter. In order to calculate S°_{298} for $Cs_2CO_3(s)$, the equilibrium constants are first converted to changes in free energy functions, $-(\Delta G^\circ_T - \Delta H^\circ_{298})/T$. The equilibrium constant is related to the change in free energy by

$$\Delta G^\circ_T = -RT\ln K_{eq} \qquad (12)$$

The change in enthalpy is calculated from data in the literature. The $\Delta H^\circ_{f,298}$ value for $Cs_2CO_3(s)$ was taken from Johnson and Gayer [7]. The $\Delta H^\circ_{f,298}$ values for $CO_2(g)$ and $H_2O(g)$ were taken from the JANAF tables [5], and the $\Delta H^\circ_{f,298}$ value for $CsOH(g)$ was taken from Cordfunke and Konings [3]. From these data the $\Delta H^\circ_{r,298}$ value for reaction (10) was calculated to be 234.62 ± 3.02 kJ/mol. From the calculated change in free energy functions, the free energy functions for $Cs_2CO_3(l)$ were calculated. The free energy functions for $CO_2(g)$ and $H_2O(g)$ were taken from the JANAF tables [5], and the free energy functions for $CsOH(g)$ were taken from Cordfunke and Konings [3]. The free energy function is given by

$$-(G^\circ_T - H^\circ_{298})/T = S^\circ_{298} + (S^\circ_T - S^\circ_{298}) - (H^\circ_T - H^\circ_{298})/T \qquad (13)$$

where

$$S^\circ_T - S^\circ_{298} = \int_{298}^{1061}(Cp(s)/T)dT + \Delta H^\circ_{fus}/1061 + \int_{1061}^{T}(Cp(l)/T)dT \qquad (14)$$

and

$$H^\circ_T - H^\circ_{298} = \int_{298}^{1061}Cp(s)dT + \Delta H^\circ_{fus} + \int_{1061}^{T}Cp(l)dT. \qquad (15)$$

Table 10. Derivation of the standard entropy for $Cs_2CO_3(s)$ from the equilibrium constants measured for the reaction.

$$1/2\ Cs_2CO_3(l) + 1/2\ H_2O(g) = CsOH(g) + 1/2\ CO_2(g) \qquad (A)$$

		reaction (A)		$Cs_2CO_3(l)$			
run #	T (K)	Keq (atm)	$-(\Delta G^\circ-\Delta H^\circ_{298})/T$ (J/mol-K)	$-(G^\circ-H^\circ_{298})/T$ (J/mol-K)	$S^\circ_T-S^\circ_{298}$ (J/mol-K)	$H^\circ_T-H^\circ_{298}$ (kJ/mol)	S°_{298} (J/mol-K)
95	1124.3	7.763×10^{-4}	149.14	303.00	251.49	182.95	214.23
96	1120.4	9.204×10^{-4}	151.28	298.41	250.81	182.19	210.21
97	1172.0	1.984×10^{-3}	148.45	307.99	259.60	192.26	212.44
98	1169.6	1.756×10^{-3}	147.84	309.02	259.20	191.79	213.80
99	1220.9	4.191×10^{-3}	146.73	315.04	267.57	201.80	212.76
100	1269.2	8.443×10^{-3}	145.15	321.67	275.14	211.23	212.95
							212.73 ± 1.41

$S^\circ_T - S^\circ_{298}$ and $H^\circ_T - H^\circ_{298}$ were then calculated for each experiment using the heat capacities for $Cs_2CO_3(s)$ given by Barin [6], the heat capacities for $Cs_2CO_3(l)$ given herein, and the heat of fusion given by Kobayasi, et al. [8]. By eqn (13), a S°_{298} value for each experiment was then obtained. The standard entropies for $Cs_2CO_3(s)$ derived in this manner are given in Table 10. Averaged the data yield 212.73 ± 1.42 J/mol-K for the $S^\circ298$ value of $Cs_2CO_3(s)$.

Activity Coefficients

Using the definition in eqn (1), activity coefficients for $Cs_2CO_3(l)$ can be calculated. For purposes of comparison with the activity coefficient of CsCl(l), the activity coefficient of $Cs_2CO_3(l)$ is given per mole of cesium, i.e. as $\gamma(Cs_2CO_3)^{1/2}$. For pure Cs_2CO_3, 13.9wt%Cs_2CO_3/Na_2CO_3, 0.2wt%Cs_2CO_3/Na_2CO_3, and 10.2wt%Cs_2CO_3/22.5wt%Na_2SO_4/Na_2CO_3, the activity coefficients for Cs_2CO_3 are derived in Table 11. The equilibrium constant, K_{eq}, was calculated using thermodynamic data from the JANAF tables [5] for $CO_2(g)$ and $H_2O(g)$, from Cordfunke and Konings [3] for CsOH(g), and from Table 1 for $Cs_2CO_3(l)$. Over the temperature range of 1100 to 1300 K, K_{eq} for reaction (10) can be fitted to the equation

$$\log K_{eq} = -0.9878(10^4/T) + 5.7170 \qquad (16)$$

where

$$K_{eq} = p(CsOH)p(CO_2)^{1/2}/p(H_2O)^{1/2}$$

and

$$a(Cs_2CO_3)^{1/2} = \gamma(Cs_2CO_3)^{1/2}y^+(Cs^+)y^-(CO_3{}^{2-})^{1/2}.$$

For pure Cs_2CO_3, $\gamma(Cs_2CO_3)^{1/2}$ was calculated to be 1.001 ± 0.088. For 13.9wt%Cs_2CO_3/ Na_2CO_3, $\gamma(Cs_2CO_3)^{1/2}$ was calculated to be 1.136 ± 0.140, and for 0.2wt%Cs_2CO_3/Na_2CO_3, $\gamma(Cs_2CO_3)^{1/2}$ was calculated to be 1.621 ± 0.588. The activity coefficients are near unity for the solutions, thus exhibiting almost ideal behavior. However, the activity coefficient of the solutions are slightly greater than unity implying a positive deviation from ideality, while the enthalpy of solution measurements in the literature [9] discussed earlier indicate a small negative deviation from ideality. At 1173 K, a plot of log K_{eq} as a function of log $x^+(Cs^+)$ is given in Figure 12.

Table 11. Activities and activity coefficients of Cs_2CO_3 in Na_2CO_3 and Na_2SO_4/Na_2CO_3 solutions.
($K^{\circ}_{eq} = p(CsOH)p(CO_2)^{1/2}/p(H_2O)_{1/2}$)

run #	T (K)	K°_{eq}	K_{eq}	$a(Cs_2CO_3)^{1/2}$	$\gamma(Cs_2CO_3)^{1/2}$
pure Cs_2CO_3, $y^{+}(Cs^{+}) = 1.0000$					
95	1124.3	7.763×10^{-4}	8.494×10^{-4}	0.9139	0.9139
96	1120.4	9.204×10^{-4}	7.908×10^{-4}	1.1640	1.1640
97	1172.0	1.984×10^{-3}	1.951×10^{-3}	1.0167	1.0167
98	1169.6	1.756×10^{-3}	1.875×10^{-3}	0.9364	0.9364
99	1220.9	4.191×10^{-3}	4.245×10^{-3}	0.9871	0.9871
100	1269.2	8.443×10^{-3}	8.566×10^{-3}	0.9857	0.9857
					1.0006 ± 0.0883
13.9wt%Cs_2CO_3, $y^{+}(Cs^{+}) = 0.05001$					
14	1220.2	2.801×10^{-4}	4.200×10^{-3}	0.06668	1.3333
15	1231.7	2.512×10^{-4}	4.994×10^{-3}	0.05031	1.0060
17	1226.8	2.782×10^{-4}	4.641×10^{-3}	0.05995	1.1988
18	1224.7	2.790×10^{-4}	4.496×10^{-3}	0.06204	1.2406
19	1124.4	4.350×10^{-5}	8.510×10^{-4}	0.05111	1.0220
20	1176.0	1.060×10^{-4}	2.085×10^{-3}	0.05075	1.0148
					1.1359 ± 0.1403
0.2wt%Cs_2CO_3, $y^{+}(Cs^{+}) = 0.0006517$					
58	1173.3	2.425×10^{-6}	1.994×10^{-3}	0.001216	1.8659
60	1173.8	1.503×10^{-6}	2.011×10^{-3}	0.0007476	1.1471
62	1221.5	7.108×10^{-6}	4.284×10^{-3}	0.001659	2.5456
64	1221.6	3.654×10^{-6}	4.291×10^{-3}	0.0008516	1.3067
66	1272.1	7.208×10^{-6}	8.918×10^{-3}	0.0008083	1.2403
					1.6211 ± 0.5880
10.2wt%Cs_2CO_3/22.5wt%Na_2SO_4, $y^{+}(Cs^{+}) = 0.03793$, $y^{-}(CO_3^{2-}) = 0.8076$					
21	1175.6	9.984×10^{-5}	2.071×10^{-3}	0.04820	1.4141*
22	1124.5	2.296×10^{-5}	8.525×10^{-4}	0.02693	0.7901
23	1125.4	1.853×10^{-5}	8.666×10^{-4}	0.02139	0.6275
25	1126.5	1.259×10^{-4}	8.842×10^{-4}	0.1424	4.1776*
27	1225.7	1.154×10^{-4}	4.565×10^{-3}	0.02529	0.7419
29	1177.4	5.250×10^{-5}	2.134×10^{-3}	0.02461	0.7220
*runs not included in average					0.7204 ± 0.0682

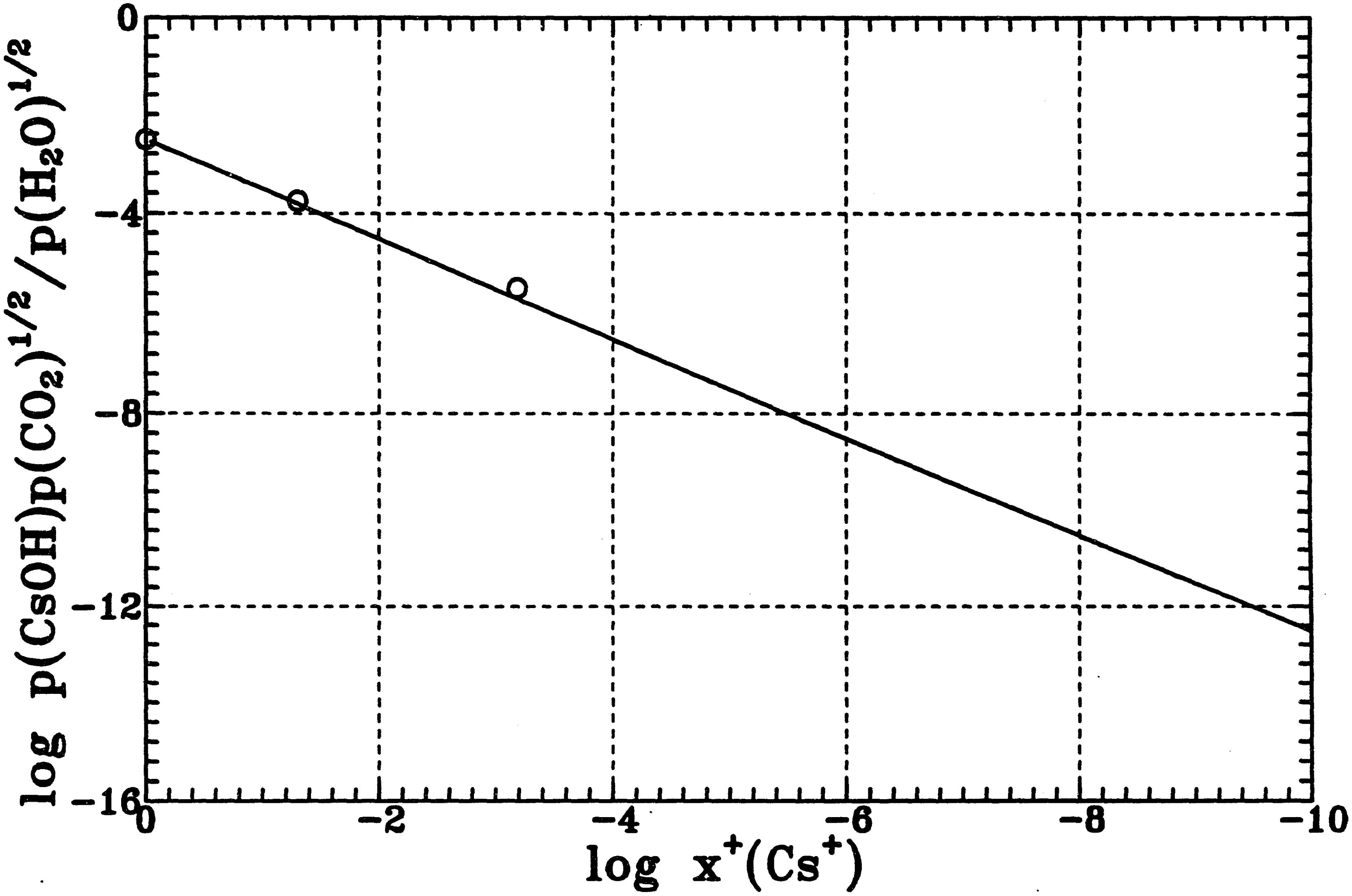

Figure 12. Plot showing log $p(CsOH)p(CO_2)^{1/2}/p(H_2O)^{1/2}$ as a function of log $x^+(Cs^+)$ at 1200 K. The solid line is the curve expected from Raoult's law.

Table 12. Activities and activity coefficients of CsCl in $NaCl/Na_2CO_3$ solutions. ($K°_{eq}$ = p(CsCl))

run #	T (K)	$K°_{eq}$	K_{eq}	a(CsCl)	γ(CsCl)
12.5wt%Cs_2CO_3/10.0wt%NaCl, $y^+(Cs^+) = 0.04502$, $y^-(Cl^-) = 0.1000$					
36	1127.9	4.844×10^{-4}	1.612×10^{-2}	0.03004	6.6726
37	1127.0	5.292×10^{-4}	1.591×10^{-2}	0.03325	7.3856
39	1082.4	3.694×10^{-4}	8.087×10^{-3}	0.04568	10.1466
41	1075.1	3.829×10^{-4}	7.195×10^{-3}	0.05323	11.8236
43	1183.1	1.003×10^{-3}	3.433×10^{-2}	0.02922	6.4904
45	1226.0	1.631×10^{-3}	5.852×10^{-2}	0.02787	6.1906
					8.1182 ± 2.3167

The solid line is the trend expected from Raoult's law and agrees well with the data. Neglecting the data from runs #21 and #29 since they deviate significantly from the other runs, $\gamma(Cs_2CO_3)^{1/2}$ for 10.2wt%Cs_2CO_3/22.5wt%Na_2SO_4/Na_2CO_3, was calculated to be 0.720 ± 0.068. (If the datum from run #21 was included, $\gamma(Cs_2CO_3)^{1/2}$ was calculated to be 0.859 ± 0.316.) Thus, a solution containing sulfate exhibits a small negative deviation from ideality.

Using the definition in eqn (3), the activity coefficient of CsCl(l) can be calculated. For 12.5wt%Cs_2CO_3/10.0wt%NaCl/Na_2CO_3, the activity coefficients are derived in Table 12. K_{eq} was calculated using the free energy functions for CsCl(l) and CsCl(g) and the $\Delta H°_{f,298}$ value for CsCl(l) given in the JANAF tables [5]. The $\Delta H°_{f,298}$ value for CsCl(g) was based on data summarized in the JANAF tables [5] for the vaporization reaction

$$CsCl(l) = CsCl(g). \qquad (11)$$

The selected $\Delta H°_{f,298}$ value for CsCl(g) was -248.42 ± 1.58 kJ/mol. Over the temperature range of 1100 to 1300 K, K_{eq} for reaction (11) can be fitted to the equation

$$\log K_{eq} = -0.7848(10^4/T) + 5.1670 \qquad (17)$$

where

$$K_{eq} = p(CsCl)/a(CsCl)$$

and

$$a(CsCl) = \gamma(CsCl)y^+(Cs^+)y^-(Cl^-).$$

For 12.5wt%Cs_2CO_3/10.0wt%NaCl/Na_2CO_3, γ(CsCl) was calculated to be 8.118 ± 2.317. Thus, a carbonate solution containing chloride exhibits a positive deviation from ideality.

Application to Molten Salt Oxidation

CsCl(g) versus CsOH(g) Cross-Over Chloride Concentration

For the molten salt oxidizer, it is useful to know the cross-over chloride concentration for dilute solutions of cesium in the NaCl(l)-Na_2CO_3(l) system where the vapor pressures of CsCl(g) and CsOH(g) are equal. At higher chloride concentrations, CsCl(g) will be the major cesium vapor species and at lower chloride concentrations CsOH(g) will be the major cesium vapor species. The calculated cross-over chloride concentration will vary with the CO_2(g) and H_2O(g) pressures. For these calculations, however, the CO_2(g) and H_2O(g) pressures are taken to be equal and the reactive gas pressure effect cancels out. (See eqn (16)) Setting the vapor pressures of CsOH(g) and CsCl(g) given by eqns (16) and (17) equal, the following equation is obtained:

$$\log y^{-}(Cl^{-})/(1 - y^{-}(Cl^{-}))^{1/2} = -0.2030(10^4/T) - 0.1497 \qquad (18)$$

where $\gamma(Cs_2CO_3)^{1/2} = 1.621$ and $\gamma(CsCl) = 8.118$. From eqn (4), the anion mole fraction of chloride is related to the anion equivalent fraction of chloride by

$$x^{-}(Cl^{-}) = 2y^{-}(Cl^{-})/(1 + y^{-}(Cl^{-})). \qquad (19)$$

For the molten salt oxidizer, the operating temperature is about 1200 K. Thus, the cross-over point is calculated to be at the chloride equivalent composition, $y^{-}(Cl^{-}) = 1.431 \times 10^{-2}$, and the chloride mole fraction, $x^{-}(Cl^{-}) = 2.821 \times 10^{-2}$. A similar calculation can be made to determine the cross-over point of NaCl(g) over NaOH(g) in the NaCl(l)-Na_2CO_3(l) system. Using the data in the JANAF tables [5] and setting the pressures of NaCl(g) and NaOH(g) equal, the cross-over chloride composition at 1200 K is calculated to be at the chloride equivalent fraction, $y^{-}(Cl^{-}) = 1.579 \times 10^{-2}$, and the chloride mole fraction, $x^{-}(Cl^{-}) = 3.109 \times 10^{-2}$, which is nearly the same as that calculated for cesium.

Calculation of Percent Retention

The thermodynamic data derived herein can now be used to calculate the percent retention of cesium in the molten salt oxidizer. The percent retention is defined as

$$\%R = 100N_m(Cs)/[N^\circ_m(Cs)+N_f(Cs)] \quad (20)$$

where $N_m(Cs)$ is the total number of moles (or grams) of cesium remaining in the melt, $N^\circ_m(Cs)$ is the initial number of moles (or grams) of cesium in the melt, and $N_f(Cs)$ is the number of moles (or grams) of cesium added in the feed. In order to calculate the percent retention, the mole fraction of cesium in the melt as a function of operating time is needed. For convenience of notation the following definitions are made:

a = moles of Cs added in feed per minute
b = moles of Cs carryover per minute total divided by $x^+(Cs^+)$
c = moles of Na carryover per minute total
$C = N^\circ_m(Na)$ = total moles Na in melt initial
t = time in minutes
$x^\circ = x^{\circ+}(Cs^+)$ = mole fraction initial of cesium in melt
$x = x^+(Cs^+)$ = mole fraction of cesium in melt

b_v = moles Cs volatilized per minute from pure $Cs_2CO_3(l)$
c_a = moles of Na added per minute
c_v = moles of Na volatilized per minute from pure $Na_2CO_3(l)$
e = moles of Na entrained per minute

The total amount of cesium carryover per minute divided by the cesium mole fraction is given by

$$b = b_v + e \quad (21)$$

and the total amount of sodium carryover per minute is given by

$$c = c_v + e - c_a \quad (22)$$

The cation mole fraction of cesium is given by

$$x = N_m(Cs)/[N_m(Cs) + N_m(Na)] \quad (23)$$

where

$$N_m(Cs) = N^\circ_m(Cs) + {}_0\int^t a - bx\, dt \quad (24)$$

and if x is small

$$N_m(Na) = N^\circ_m(Na) - {}_0\int^t c\, dt \quad (25)$$

Substitution of eqns (24) and (25) into eqn (23), assuming x is small, yields

$$x = \left[{}_0\int^t a - bx\, dt\right]/\left[C - {}_0\int^t c\, dt\right] \tag{26}$$

Eqn (26) can be rewritten as the differential equation

$$(C - ct)dx/dt + (b - c)x - a = 0.0. \tag{27}$$

The solution to this equation is given as

$$x = v + (x^\circ - v)(1 + u)^{-w} \tag{28}$$

where

$u = ct/(C - ct)$,

$v = a/(b - c)$,

and

$w = (b - c)/c$.

If the net carryover of sodium is zero, i.e. $c = 0$, then the solution to eqn (28) becomes

$$x = v + (x^\circ - v)e^{-bt/C}. \tag{29}$$

To calculate percent retention, x is then converted to $N_m(Cs)$, $N^\circ{}_m(Cs)$, and $N_f(Cs)$ by the relationships

$$N_m(Cs) = (C - ct)x, \tag{30}$$

$$N^\circ{}_m(Cs) = Cx, \tag{31}$$

and

$$N_f(Cs) = at, \tag{32}$$

and then substituted into eqn (20). In addition, the total number of moles of cesium carryover, $N_c(Cs)$, is given by

$$N_c(Cs) = N^\circ_m(Cs) + N_f(Cs) - N_m(Cs) \qquad (33)$$

Application to the Rockwell MSO Process

Eqn (28) (or eqn (29) when $c = 0$) can be used to calculate the percent retention of cesium in the molten salt oxidizer. The following are taken to be the operating conditions: $p(H_2O) = p(CO_2)$ (approximately 0.1 atm each), a total pressure of 1 atmosphere, a salt entrainment rate of 1 pound per day, a salt addition rate of 1 pound per day, an offgas flow rate of 3.0 standard cubic feet per minute (SCFM) when wet, a cesium feed rate of 3.0×10^{-7} g Cs per day, a bath size of about 12 pounds of salt, an initial cesium concentration equal to zero, and an operating temperature of 1200 K. Three different bath compositions are considered, pure Na_2CO_3, 20wt%Na_2SO_4 in Na_2CO_3, and 10.0wt%NaCl in Na_2CO_3.

From these conditions, the moles of Na physically entrained per minute, e, becomes 5.944×10^{-3}. The moles of Na added per minute, c_a, becomes 5.944×10^{-3}. The total moles of Na initial in the melt, C, becomes 102.7. (All are based on a pure Na_2CO_3 melt. The same Na physical entrainment rate, Na addition rate, and number of total initial moles of sodium are taken for the 20wt%Na_2SO_4 in Na_2CO_3 and the 10wt%NaCl in Na_2CO_3 melts) The cesium feed rate, a, in moles per minute becomes 1.568×10^{-12}. Using the ideal gas equation, the cesium and sodium volatilization rates in moles per minute are given by

$$bx = 3.518(p(CsCl) + p(CsOH)) \qquad (34)$$

and

$$c = 3.518(p(NaCl) + p(NaOH)) \qquad (35)$$

where the partial pressures of CsCl(g), CsOH(g), NaCl(g), and NaOH(g) are in atm and are given by

$$p(CsOH) = p^\circ(CsOH)\gamma(Cs_2CO_3)^{1/2}y^-(CO_3^{2-})^{1/2}y^+(Cs^+), \qquad (36)$$

$$p(CsCl) = p^\circ(CsCl)\gamma(CsCl)y^-(Cl^-)y^+(Cs^+), \qquad (37)$$

$$p(NaOH) = p^\circ(NaOH)\gamma(Na_2CO_3)^{1/2}y^-(CO_3^{2-})^{1/2}y^+(Na^+), \qquad (38)$$

and

and

$$p(\mathrm{NaCl}) = p^\circ(\mathrm{NaCl})\gamma(\mathrm{NaCl})y^-(\mathrm{Cl}^-)y^+(\mathrm{Na}^+). \qquad (39)$$

If the chloride concentration is much less than 3 mol%, then the cesium and sodium volatilization rate are determined solely from the partial pressures of CsOH(g) and NaOH(g), respectively. If the chloride concentration is much greater than 3 mol%, then the cesium and sodium volatilization rates are determined solely from the partial pressures of CsCl(g) and NaCl(g), respectively. At 1200 K, eqns (16) and (17) and data in the JANAF tables [5] can be used to calculate the following: $p^\circ(\mathrm{CsOH}) = 3.072\times10^{-3}$, $p^\circ(\mathrm{CsCl}) = 4.258\times10^{-2}$, $p^\circ(\mathrm{NaOH}) = 5.065\times10^{-5}$, and $p^\circ(\mathrm{NaCl}) = 3.182\times10^{-3}$. The parameters, $y^+(\mathrm{Na}^+)$, $\gamma(\mathrm{Na_2CO_3})^{1/2}$, and $\gamma(\mathrm{NaCl})$, are taken to be equal to unity. The parameter, $y^+(\mathrm{Cs}^+)$, is equal to x.

If the starting composition of the bath is pure $\mathrm{Na_2CO_3}$, then $y^-(\mathrm{CO_3}^{2-})^{1/2}$ is 1.000 and $\gamma(\mathrm{Cs_2CO_3})^{1/2} = 1.621$. The Cs and Na volatilization rates, b_V and c_V, are calculated to be 1.752×10^{-2} mol/min and 1.782×10^{-4} mol/min, respectively. If the starting composition of the bath is 20wt%$\mathrm{Na_2SO_4}$ in $\mathrm{Na_2CO_3}$, then $y^-(\mathrm{CO_3}^{2-})^{1/2}$ is 0.9180 and $\gamma(\mathrm{Cs_2CO_3})^{1/2}$ is 0.720. The Cs and Na volatilization rates, b_V and c_V, are calculated to be 7.147×10^{-3} mol/min and 1.636×10^{-4} mol/min, respectively. If the starting composition of the bath is 10.0wt%NaCl in $\mathrm{Na_2CO_3}$, then $y^-(\mathrm{Cl}^-)$ is 0.09153 and $\gamma(\mathrm{CsCl})$ is 8.118. The Cs and Na volatilization rates, b_V and c_V, are calculated to be 1.113×10^{-1} mol/min and 1.024×10^{-3} mol/min, respectively.

The percent retention as a function of time for each of the three melt compositions, $\mathrm{Na_2CO_3}$, 20wt%$\mathrm{Na_2SO_4/Na_2CO_3}$, and 10wt%$\mathrm{NaCl/Na_2CO_3}$, is shown in Figure 13. Over a 25 hour period, 20wt%$\mathrm{Na_2SO_4/Na_2CO_3}$ is calculated to have the best retention, about 91.0%. $\mathrm{Na_2CO_3}$ is calculated to have a slightly worse retention, about 84.6%, and 10wt%$\mathrm{NaCl/Na_2CO_3}$ is calculated to have very poor retention, about 47.5%. The total amounts of cesium volatilized are calculated to be 1.53×10^{-8} g, 3.58×10^{-8} g, and 1.56×10^{-7} g and the total amounts of cesium physically entrained are calculated to be 1.28×10^{-8} g, 1.22×10^{-8} g, 8.31×10^{-9} g for 20wt%$\mathrm{Na_2SO_4/Na_2CO_3}$, $\mathrm{Na_2CO_3}$, and 10wt%$\mathrm{NaCl/Na_2CO_3}$, respectively.

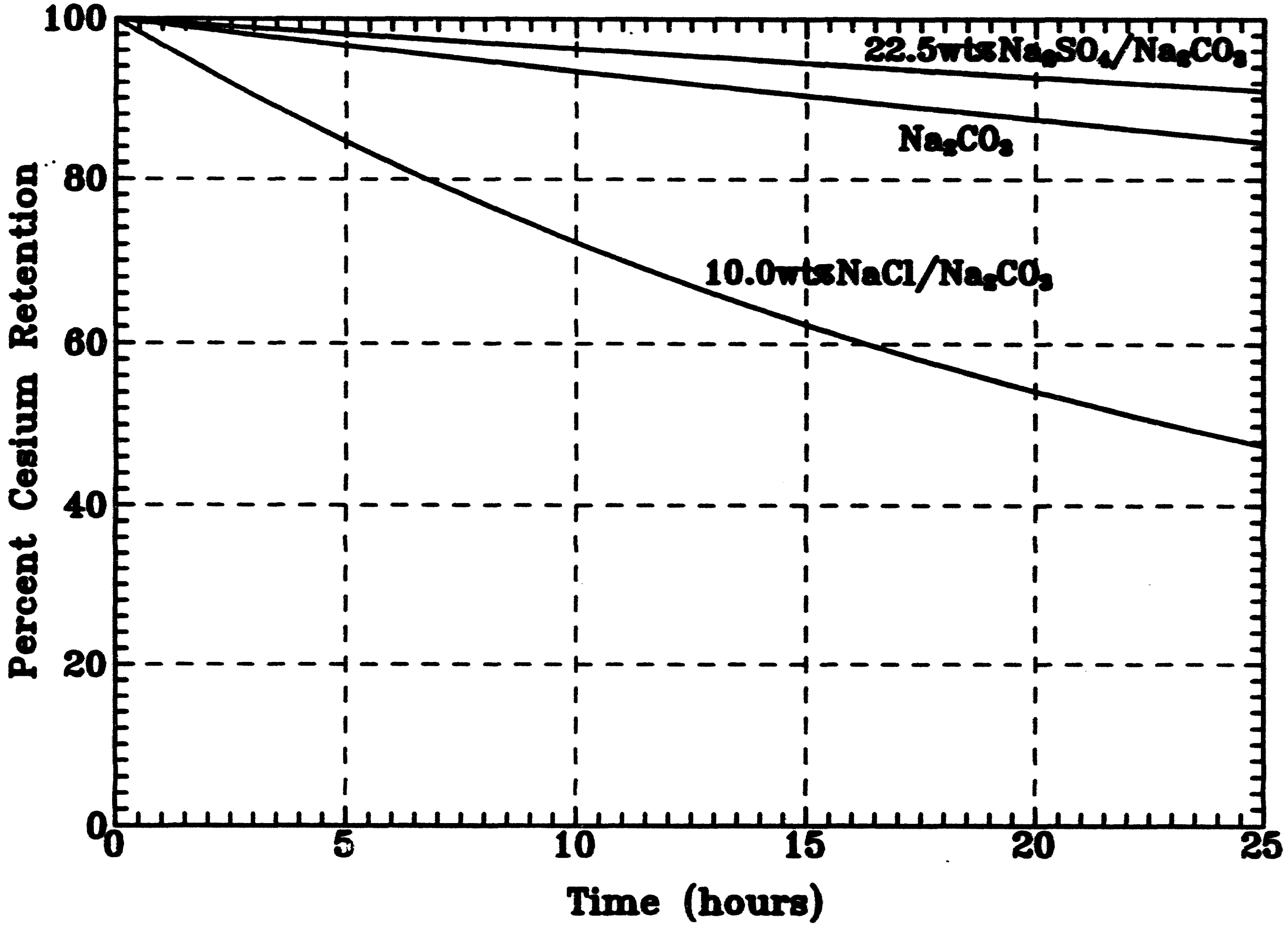

Figure 13. Plot showing calculated percent retention of cesium in the molten salt oxidizer as a function of time in hours for initial molten salt compositions of pure Na_2CO_3, 20wt%Na_2SO_4/Na_2CO_3, and 10wt%NaCl/Na_2CO_3 at equal pressures of H_2O(g) and CO_2(g), a bath temperature of 1200 K, an offgas flow rate of 3.0 SCFM (wet), a cesium feed rate of 3.0×10^{-7} g/day, a bath size of 12 lbs, and a salt physical entrainment rate and a salt addition rate of 1 lb/day.

conditions except for the parameter which is varied are the same as given above and the time of operation is 25 hours. If the offgas flow rate is varied from 2.0 SCFM (wet) to 4.0 SCFM (wet), the percent cesium retention varies from 88.2% to 81.3%. If the salt physical entrainment rate and addition rate vary from 0.5 lb/day to 1.5 lb/day, the percent retention varies from 86.4% to 82.9%. If the operating temperature varies from 1125 to 1275 K, the percent retention varies from 92.5% to 66.9%. If the initial concentration of cesium in the bath is increased from zero, the percent retention is decreased from 84.6% and levels off at 71.0% for higher initial concentrations of cesium. If the cesium feed rate is varied, the percent retention remains constant at 84.6%. Similar trends are expected for the 20wt%Na_2SO_4/Na_2CO_3 and 10wt%NaCl/Na_2CO_3 baths.

Summary and Conclusions

Transpiration experiments have been applied to determine the volatility of cesium from molten carbonate mixtures at temperatures ranging from 1073 to 1373 K. The major cesium vapor species is determined to be CsOH(g) except when greater than about 3 mol% chloride is present in the melt, then the major cesium vapor species is CsCl(g). The activity coefficient of cesium carbonate, $\gamma(Cs_2CO_3)^{1/2}$, in solutions containing Cs_2CO_3 and Na_2CO_3 is determined to be near unity, 1.00 for pure Cs_2CO_3 and 1.62 for infinitely dilute concentrations of Cs_2CO_3. The addition of about 20 wt% Na_2SO_4 to the bath reduces the cesium volatility by about a factor of 2, and the addition of about 10 wt% NaCl to the bath increases the cesium volatility by about a factor of 10. The activity coefficient of cesium carbonate, $\gamma(Cs_2CO_3)^{1/2}$, in a solution containing 10.2wt% Cs_2CO_3, 22.5wt% Na_2SO_4, and 67.3wt% Na_2CO_3 is determined to be 0.72, and the activity coefficient of cesium chloride, γ(CsCl), in a solution containing 12.5wt% Cs_2CO_3, 10.0wt% NaCl, and 77.5wt% Na_2CO_3 is determined to be 8.11. The addition of up to 2 wt% ash or silica has no effect on cesium volatility. The addition of 2 wt% molecular sieve 5A seems to reduce the cesium volatility but only at higher temperatures, i.e. around 1373 K.

The thermodynamic data have been applied to the Rockwell molten salt oxidizer. Taking the pressures of H_2O(g) and CO_2(g) to be equal, the total pressure to be 1 atmosphere, the salt entrainment rate and the salt addition rate to each be 1 pound per day, the offgas flow rate to be 3.0 standard cubic feet per minute (wet), the cesium feed rate to be 3.0×10^{-7} grams per day, the bath size to be 12 pounds of salt, the initial cesium concentration to be equal to zero, and the operating temperature to be

1200 K, the percent cesium retention for the salt compositions, pure Na_2CO_3, 20wt% Na_2SO_4 in Na_2CO_3, 10wt% NaCl in Na_2CO_3, are calculated as a function of operating time. The melt 20wt%Na_2SO_4/Na_2CO_3 is calculated to have the best cesium retention, about 91.0% after 25 hours of operation, and the melt 10wt%NaCl/Na_2CO_3 is calculated to have the worst cesium retention, about 47.5% after 25 hours of operation. Pure Na_2CO_3 was calculated to have a retention of about 84.6% after 25 hours of operation. The percent retention of cesium is increased by lower operating temperatures, by lower salt physical entrainment rates, by lower offgas flow rates, and by the presence of sulfate in the bath. However, the cesium feed rate has no effect on the calculated retention of cesium.

Acknowledgements

We gratefully acknowledge the assistance provided by Charles H. Otto, Jr., for the cesium analyses.

References

1. Molten Salt Oxidation Technology-Progress Report, DOE/ID/12584-119, May, 1993.

2. L. F. Grantham, D. E. McKenzie, W. L. Richards, R. D. Oldenkamp, Molten Salt Combustion of Radioactive Wastes, *Proc. ERDA Air Clean Conf.*, **14**, 17-35, 1976.

3. E. H. P. Cordfunke, R. J. M. Konings, P. E. Potter, G. Prins, and M. H. Rand, Thermochemical Data for Reactor Materials and Fission Products, editors E. H. P. Cordfunke and R. J. M. Konings, North Holland, Amsterdam, 1990.

4. R. H. Lamoreaux and D. L. Hildebrand, "High Temperature Vaporization Behavior of Oxides. I. Alkali Metal Binary Oxides," *J. Phys. Chem. Ref. Data*, **13**, 151-173 (1984).

5. M. W. Chase, Jr., C. A. Davies, J. R. Downey, Jr., D. J. Frurip, R. A. McDonald, and A. N. Syverund, JANAF Thermochemical Tables, 3rd Edition, Parts I and II (*J. Phys Chem. Ref. Data*, **14**, 1985, Supplement No. 1), American Chemical Society and American Institute of Physics, New York, 1986.

6. I. Barin, Thermochemical Data of Pure Substances, VCH, New York, 1989.

7. G. K. Johnson and K. H. Gayer, "The Enthalpies of Solution and Formation of Cs_2CO_3," *J. Chem. Thermo.*, **12**, 705-708 (1980).

8. K. Kobayasi, N. Inoue, and T. Takano, "Specific Heat of Solid and Molten Phases, and Latent Heat of Fusion of Some Carbonates," *Netsu Bussei*, **6**, 2-7 (1992).

9. B. K. Andersen and O. J. Kleppa, "Enthalpies of Mixing in Binary Liquid Alkali Carbonate Mixtures," *Acta Chem. Scand. A*, **30**, 751-758 (1976).

10. T. Ostvold and O. J. Kleppa, "Enthalpies of Mixing in Binary Liquid Alkali Sulfate Mixtures," *Acta Chem. Scand.*, **25**, 919-929 (1971).

11. L. S. Hersh and O. J. Kleppa, "Enthalpies of Mixing in Some Binary Liquid Halide Mixtures," *J. Chem. Phys.*, **42**, 1309-1322 (1965).

12. Y. Dessureault, J. Sangster, and A. D. Pelton, "Coupled Phase Diagram-Thermodynamic Analysis of the 24 Binary Systems, A_2CO_3-AX and A_2SO_4-AX Where A = Li. Na, K and X = Cl, F, NO_3, OH," *J. Phys. Chem. Ref. Data*, **19**, 1149-1178 (1990).

13. C. W. Bale and A. D. Pelton, "Coupled Phase Diagram and Thermodynamic Analysis of the 18 Binary Systems Formed Among Li_2CO_3, K_2CO_3, Na_2CO_3, LiOH, KOH, NaOH, Li_2SO_4, K_2SO_4, and Na_2SO_4," *CALPHAD*, **6**, 255-278 (1982).

14. F. D. Richardson and C. B. Alcock, "Chemical Equilibria," in Physiochemical Measurements at High Temperatures, edited by J. O'M. Bockris, J. L. White, and J. D. Mackenzie, Butterworths Sci. Publ., London, 1959, pp 135-170.

15. O. H. Krikorian, B. B. Ebbinghaus, M. G. Adamson, A. S. Fontes, Jr., D. L. Fleming, "Experimental Studies and Thermodynamic Modeling of Volatilities of Uranium, Plutonium, and Americium from Their Oxides and from Their Oxides Interacted with Ash," Lawrence Livermore National Laboratory Report, UCRL-ID-114774, Sept. 15, 1993.

DATE
FILMED

6/29/94

END